Eckman

NOAA Technical Memorandum ERL ARL - 193

PRELIMINARY ANALYSIS OF WIND DATA FROM THE OAK RIDGE SITE SURVEY

Richard M. Eckman
Ronald J. Dobosy
William R. Pendergrass

Air Resources Laboratory
Silver Spring, Maryland
February 1992

noaa NATIONAL OCEANIC AND ATMOSPHERIC ADMINISTRATION / Environmental Research Laboratories

NOAA Technical Memorandum ERL ARL - 193

PRELIMINARY ANALYSIS OF WIND DATA FROM THE OAK RIDGE SITE SURVEY

Richard M. Eckman
Ronald J. Dobosy
William R. Pendergrass
Atmospheric Turbulence and Diffusion Division
Oak Ridge, Tennessee

Air Resources Laboratory
Silver Spring, Maryland
February 1992

ATDD Contribution File no. 91/27

NOTICE

Mention of a commercial company or product does not constitute an endorsement by NOAA/ERL. Use for publicity or advertising purposes, of information from this publication concerning proprietary products or the tests of such products, is not authorized.

For sale by the National Technical Information Service
5285 Port Royal Road, Springfield, VA 22161

CONTENTS

LIST OF FIGURES

LIST OF TABLES

PRELIMINARY ANALYSIS OF WIND DATA FROM THE OAK RIDGE SITE SURVEY

Richard M. Eckman, Ronald J. Dobosy,* and William R. Pendergrass

ABSTRACT. From October 1989 until the end of 1990, the Atmospheric Turbulence and Diffusion Division (ATDD) conducted a meteorological site survey of the area around Oak Ridge, Tennessee. Twenty-eight meteorological towers were used to obtain one-minute and 15-minute averages of wind speed, wind direction, temperature, relative humidity, and rainfall. A preliminary analysis of the wind data from this survey is presented in this report. The analysis indicates that approximately eight meteorological towers can provide adequate coverage of the regional-scale surface winds around Oak Ridge when the wind speed exceeds $2\,\mathrm{m\,s^{-1}}$. For wind speeds of 0.5 to $2\,\mathrm{m\,s^{-1}}$, roughly 16 towers can adequately resolve the along-valley component of the surface wind, but the cross-valley component requires an impractical number of towers to be resolved in these light winds. The towers should be located either on local ridge tops or in local valley bottoms. Ridge-top sites should be roughly 16–18 km apart, whereas valley-bottom sites should be about 6–8 km apart. The U.S. Department of Energy (DOE) already has three meteorological measurement sites in the Oak Ridge area. To provide better coverage of the regional wind field, ATDD has produced a list of ten recommended sites for supplemental towers. Five of the recommended sites are on ridge tops, and four are in valley bottoms. The tenth site is in the Cumberland Mountains to the west of Oak Ridge. The ridge-top sites have an average separation of about 20 km, and the valley-bottom sites have an average separation of 8 km.

1. INTRODUCTION

The U.S. Department of Energy operates six nuclear-material plants that fall under the jurisdiction of Oak Ridge Operations (ORO), which is headquartered in Oak Ridge, Tennessee. Three of these plants are located on the Oak Ridge Reservation, whereas the others are near Fernald, Ohio; Portsmouth, Ohio; and Paducah, Kentucky. All of the plants store chemicals that could produce a toxic atmospheric cloud during an accident. Although each plant had independently developed a capability to model and deal with hazardous atmospheric releases, ORO decided in 1986 to upgrade and integrate its emergency-response capability. Part of the upgrade involves the development and implementation of improved computer models for simulating atmospheric diffusion.

* Affiliated with Oak Ridge Associated Universities

The Atmospheric Turbulence and Diffusion Division (ATDD), which is also located in Oak Ridge but is part of the National Oceanic and Atmospheric Administration (NOAA), has been given the task of upgrading ORO's ability to deal with accidental releases of hazardous materials. The ATDD emergency-management program has two components. One component has concentrated on developing improved computer models for simulating atmospheric diffusion during accidents (Eckman and Dobosy, 1989; Eckman, 1990; ATDD, 1991). The other component has conducted meteorological site surveys at each of the ORO plants (*e.g.*, Pendergrass, 1989). These site surveys provide information on the spatial and temporal distribution of winds, temperature, and other meteorological variables at the various plant sites. The wind measurements are used to improve the computer simulations of atmospheric diffusion and to provide recommendations to ORO on how many meteorological towers should permanently be installed around each plant.

The site surveys at Fernald, Paducah, and Portsmouth were conducted in 1987 and 1988. During each survey, from 14 to 20 meteorological towers were placed around each plant. Data were collected for about three weeks. Preliminary reports on these site surveys have already been produced (Pendergrass, 1989, 1990a, 1990b). The main goal of these preliminary reports was to recommend how many permanent meteorological towers should be located at each plant.

In this report a preliminary analysis of wind data from the Oak Ridge site survey is presented. This survey began in the fall of 1989 and ended in December 1990. Since the three Oak Ridge plants are relatively close together, ATDD conducted one meteorological survey for the entire Oak Ridge Reservation. This survey covered a significantly larger area than the previous ones, so a larger number of towers was required. In addition, the Oak Ridge survey's duration was much longer than those of the earlier surveys. Like the preliminary reports from the earlier site surveys, the primary goal of this report is a recommendation on the number and general location of permanent meteorological towers.

In section 2 of this report, a brief characterization of the terrain around Oak Ridge is given. Section 3 describes the experimental design of the Oak Ridge site survey. Both the placement of towers and the meteorological instruments are discussed in this section. In section 4, some basic features of the wind field over the Oak Ridge Reservation are presented. Section 5 discusses the spatial correlation of the horizontal wind components. The performance of simple wind-field interpolation models is evaluated in section 6. Finally, sections 7 and 8 present conclusions and recommendations based on the data analysis.

2. DESCRIPTION OF THE OAK RIDGE AREA

2.1. Topography

The Oak Ridge Reservation covers an area of approximately 140 km^2 in the Tennessee River Valley of eastern Tennessee. This valley is 60 to 70 km wide in the Oak Ridge area, and it drains from northeast to southwest. The valley bottom is approximately 250 m MSL; it is corrugated by a series of roughly 100 m high ridges that also run from northeast to southwest (Fig. 1). To the east, the valley wall is formed by the Great Smoky Mountains (not visible in Fig. 1), which rise to elevations of about 2000 m MSL. To the west, the Cumberland Mountains rise to elevations of 1000 m MSL. Oak Ridge is close to the western side of the Tennessee River Valley.

Figure 2 is a contour map of the Oak Ridge area. Some of the 100 m ridges are still visible in this figure. The three ORO plants located on the Oak Ridge Reservation are also shown. They are designated X-10 (Oak Ridge National Laboratory), K-25 (formerly the Oak Ridge Gaseous Diffusion Plant), and Y-12. All three plants are primarily located in local valley bottoms. The major population area near the reservation is the city of Oak Ridge, which has a population of approximately 27,000 and comes within a kilometer of the Y-12 plant. Knoxville, Tennessee is approximately 30 km southeast of the reservation. Several smaller towns are also within 20 km of the reservation.

Most of the ridges on the reservation are heavily wooded with deciduous forest. Pines are also mixed in. The valley bottoms contain some forest, but are mostly open fields or developed areas. Overall, the Oak Ridge Reservation is more heavily wooded than surrounding areas.

2.2. Local Climate

East Tennessee has a temperate climate that is significantly affected by the local terrain. Average monthly temperatures at ATDD range from about 3°C in January to 25°C in July. Local terrain features can cause significant spatial deviations from these averages. The average yearly precipitation is about 139 cm, with 26 cm of snow on average. Winds are often light over the Oak Ridge Reservation; no month has average wind speeds greater than 3 $m\,s^{-1}$. Both the Tennessee River Valley and the local 100 m ridges tend to channel the wind into southwesterly and northeasterly directions.

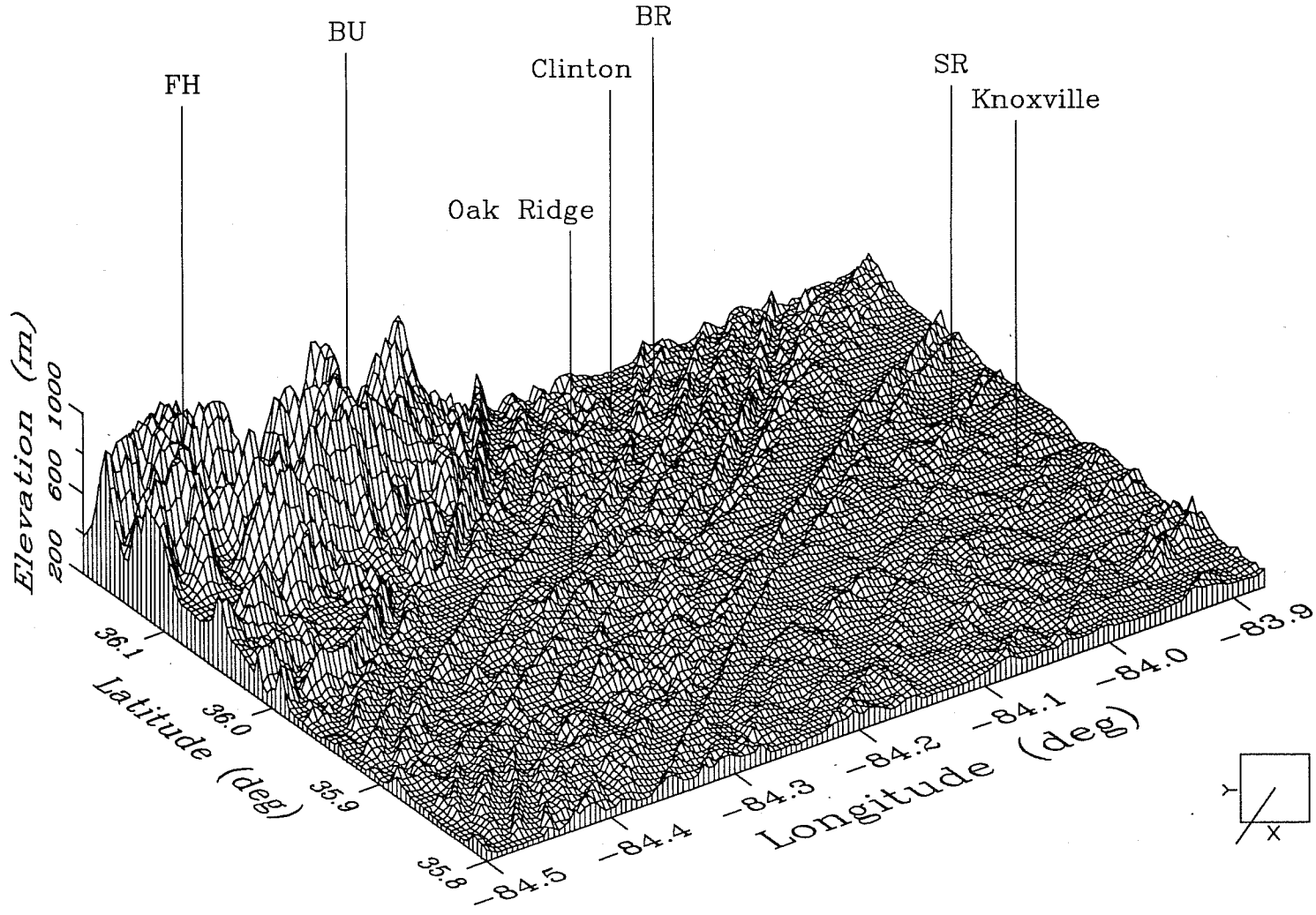

Fig. 1. Surface plot of the terrain around Oak Ridge, Tennessee. The terrain is vertically exaggerated by a factor of about 13. The locations of meteorological sites BU, BR, FH, and SR are indicated.

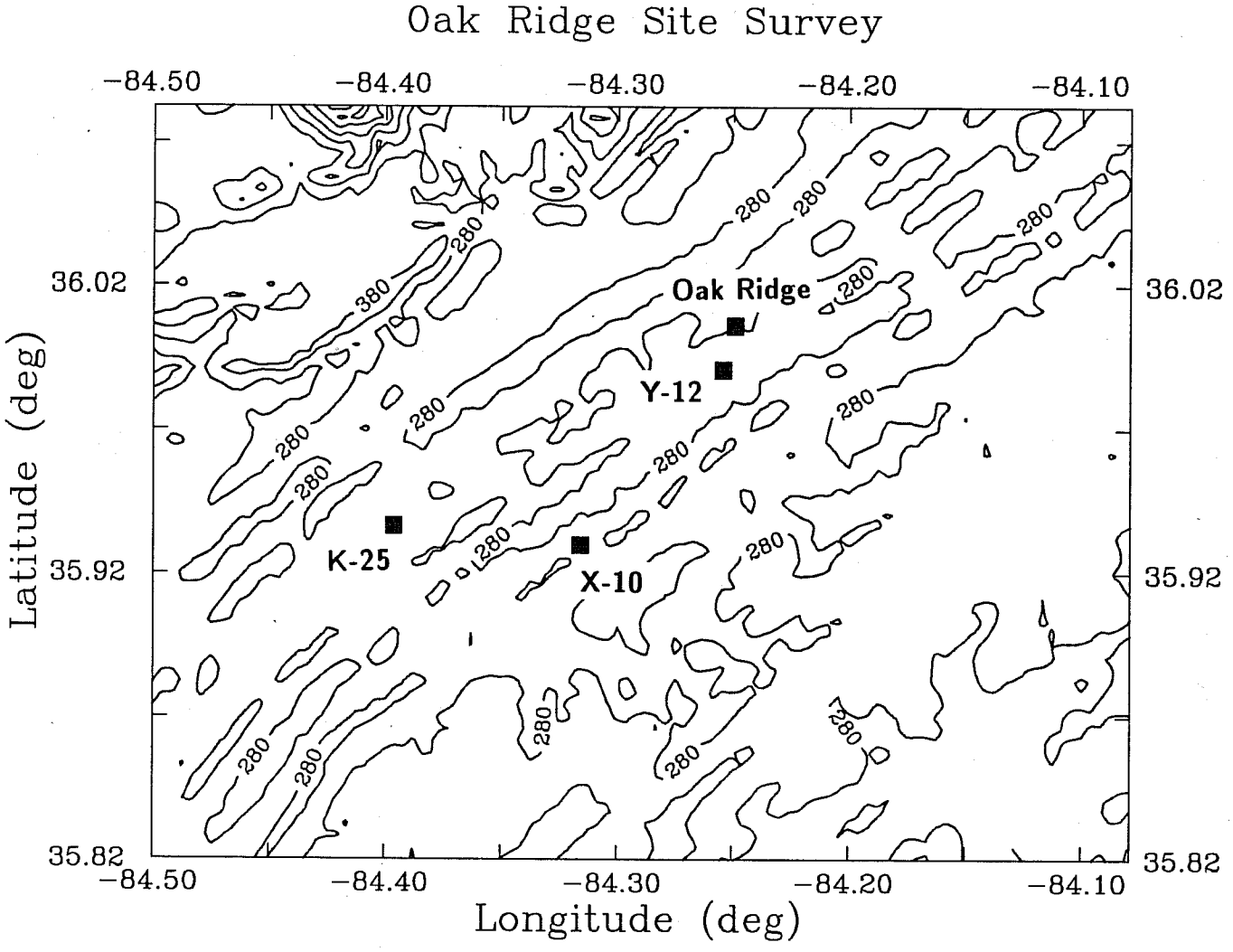

Fig. 2. Contour map of the Oak Ridge area showing the locations of the Y-12, X-10, and K-25 plants. The contours are in 100 m intervals.

3. DESCRIPTION OF THE SITE SURVEY

3.1. Data Acquisition System

The instruments used for the Oak Ridge site survey were the same as those used in the earlier surveys at Fernald, Paducah, and Portsmouth. At most sites in the Oak Ridge network the instruments were mounted on 10 m aluminum towers (Fig. 3). Other sites used pre-existent fire lookout towers and taller meteorological towers.

The instruments at each site included an R. M. Young Co. Wind Monitor–AQ, a Campbell Scientific Inc. Model 207 temperature and relative humidity probe, and a Texas Electronics Inc. Model 525 tipping bucket rain gauge. The Wind Monitor has a

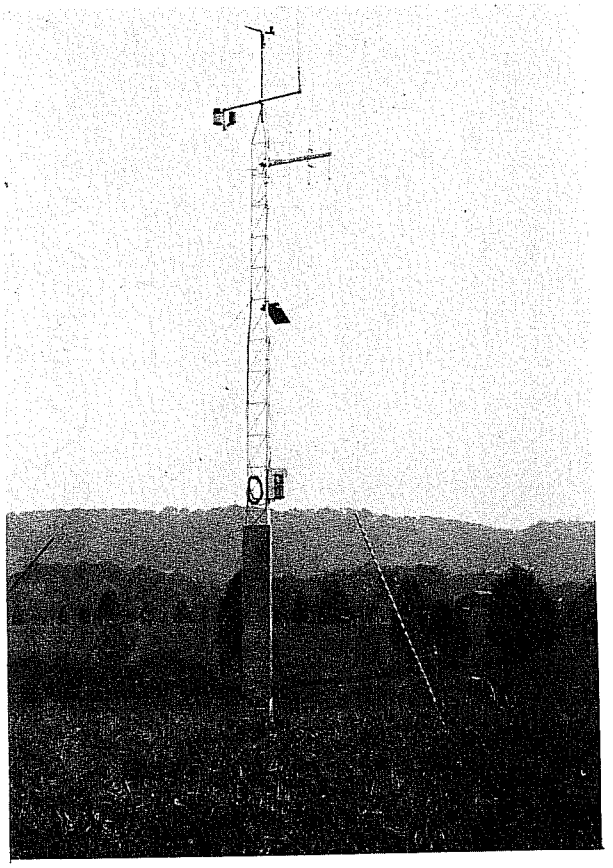

Fig. 3. An example of the 10 m aluminum towers that were used during the Oak Ridge site survey.

propeller threshold of $0.4\,m\,s^{-1}$ and a vane threshold of $0.5\,m\,s^{-1}$ for a 10° change in the wind direction. (The vane threshold is a function of the wind-direction change.) Three sites had a LI-COR Inc. Model LI-200SB pyranometer for measuring direct solar radiation and diffuse sky radiation. Six sites had a wetness sensor which provided information on the dampness of exposed surfaces.

A Campbell Scientific Inc. Model 21X Micrologger was located at each site to process raw data from the instruments. Processed data from the data logger were sent by a radio-frequency link to a base station located at ATDD, where the data were archived on Iomega Corp. Bernoulli Drive II disk cartridges. A rechargeable battery pack provided electrical power for the tower, and a solar panel was used to recharge the battery pack.

Most of the survey instruments had a sampling frequency of 1 Hz. The 21X Microloggers created sets of one-minute and 15-minute averages from the 1 Hz data. Tables 1 and 2 show the variables that are included in each set. Only the averages of the measured variables are included in the one-minute data. The 15-minute data contains both averages and standard deviations. These standard deviations were computed directly from the 1 Hz data, not from the one-minute averages.

An error was recently discovered in the way the site-survey system computed one-minute-average wind speeds and directions. The 21X Micrologger had inadvertently been programmed to compute scalar averages of the speed and direction instead of a vector average of the horizontal components. Thus, the one-minute winds may contain significant errors when fluctuations in the wind direction are large over a one-minute

Table 1. One-minute averages archived during the Oak Ridge site survey

Number	Variable	Units
1	Station number	—
2	Julian day	—
3	Time	EST
4	Wind speed	$m\,s^{-1}$
5	Wind direction	degrees
6	Temperature	°C
7	Relative humidity	%
8	Rainfall	in
9	Wetness	V
10	Solar radiation	Wm^{-2}

Table 2. Fifteen-minute averages archived during the Oak Ridge site survey. The abbreviation S.D. denotes a standard deviation

Number	Variable	Units
1	Station number	—
2	Julian day	—
3	Time	EST
4	Scalar-average wind speed	$m\,s^{-1}$
5	Magnitude of wind vector	$m\,s^{-1}$
6	Wind direction	degrees
7	S.D. wind direction	degrees
8	S.D. wind speed	$m\,s^{-1}$
9	Temperature	°C
10	S.D. temperature	°C
11	Relative humidity	%
12	S.D. relative humidity	%
13	Battery voltage	V
14	Rainfall	in
15	Minimum wind speed	$m\,s^{-1}$
16	Maximum wind speed	$m\,s^{-1}$
17	Minimum wind direction	degrees
18	Maximum wind direction	degrees
19	Minimum temperature	°C
20	Maximum temperature	°C
21	Wetness	V
22	Solar radiation	Wm^{-2}

period. Since this error cannot be reversed, the one-minute wind data must be regarded as suspect. Fortunately, the 15-minute wind averages were computed correctly.

3.2. Site Survey Network

The number of meteorological towers in the Oak Ridge network gradually increased over the course of the site survey. Thirteen sites began operation on 1 October 1989, and 28 sites were in operation by 15 November 1990. Table 3 gives information regarding each site. Figure 4 shows the location of most of the towers in the network. Sites BR, BU, FH, and SR do not appear on this map, but they are shown in Fig. 1. The sites were chosen to provide representative samples of the wind field both within the valleys and at the ridge tops. But the extensive forest cover and access problems limited the number of ideal sites for meteorological measurements. In some instances ATDD had no choice but to place towers at non-ideal sites, because better sites were not accessible.

For brevity, each of the sites listed in Table 3 is given an abbreviation. Each site also had one or more radio-frequency channel numbers assigned to it during the survey. These channel numbers are used to identify the sites in the archived data sets, so they are listed in the appendix.

Site BT in Fig 4 is a 100 m tower that was associated with a discontinued breeder-reactor program. ATDD placed six instrument sets at different levels on this tower. The measurements from the breeder site were the same as those from the other sites, but the breeder measurements were stored in a slightly different format.

In addition to the tower network, ATDD used other instrument systems to provide information about the vertical distribution of meteorological variables. From September to December 1990, a REMTECH Doppler sodar operated at either the Y-12 plant or the K-25 plant. This sodar provided wind profiles up to approximately 500 m AGL. During August and September 1990, tethered-balloon soundings were conducted at several locations on the Oak Ridge reservation. These balloons provided vertical profiles of wind, temperature, and humidity up to about 600 m AGL. Usually, the balloons provided hourly soundings over a six to eight hour period. Because of time constraints, neither the sodar nor the tethered-balloon data were analyzed for this report.

In late February and early March 1990, the Department of Energy program called Atmospheric Studies in Complex Terrain (ASCOT) conducted a field experiment in the Oak Ridge area. The ASCOT experiment's goals were to provide information on the mesoscale wind field and on the coupling between the upper-level winds and the surface winds. The experiment was coordinated with the Oak Ridge site survey to ensure that the ASCOT and site-survey measurements were complementary. ASCOT participants employed tethered balloons, pilot balloons, rawinsondes, acoustic sounders, laser anemometers, and other instruments to obtain wind measurements. These additional data are becoming available to the ATDD site survey as the ASCOT scientists edit and

Table 3. Meteorological measurement sites used during the Oak Ridge site survey. The Universal Transverse Mercator (UTM) coordinates are in zone 16

Abbreviation	Name	UTM (km) Easting	UTM (km) Northing	Measurement Heights (m AGL)	Start date
AT1	ATDD†	748.00	3987.54	17	10/1/89
AT2	ATDD†	748.00	3987.54	15	10/1/89
BR	Bluebird Ridge	764.15	4003.23	21	10/1/89
BT	Breeder tower	736.85	3974.23	11,30,46, 53,76,95	Varied
BU	Buffalo Mountain	739.77	3999.23	10	10/1/89
CF	Coalfield	729.77	3989.15	10	12/1/89
EF	East Fork	739.70	3983.80	10	11/8/90
FB	Federal Building	749.08	3990.00	15	10/8/89
FH	Frozen Head	728.81	4000.31	15,21	10/1/89
K25	K-25	735.00	3978.85	10	10/1/89
KI	Kingston plant	725.15	3976.31	10	1/27/90
KR	Kingston ridge top	729.80	3969.10	10	7/10/90
LA	Lakeside Grill	752.69	3992.85	10	2/7/90
LC	Lenoir City	741.00	3969.31	21	10/1/89
LV	Lawnville valley	730.80	3975.20	10	7/11/90
MH	Melton Hill	747.10	3974.45	10	10/15/90
OR	ORAU	746.69	3988.31	15	10/1/89
PC	Poplar Creek	738.10	3985.90	10	10/19/90
PS	Pellissippi State	755.92	3981.62	10	2/6/90
PV	Powell valley	760.80	3986.60	10	10/16/90
SA	Sludge Area	739.23	3979.54	10	12/15/89
SC	Scarboro	750.73	3985.46	10	10/1/89
SR	Sharp's ridge	775.40‡	3988.23‡	21	10/1/89
WB	Walker Branch	744.62	3982.62	45	10/1/89
WP	Water plant	735.69	3976.92	10	10/1/89
X10	X-10 gap	742.00	3980.46	10	3/6/90
25R	K-25 ridge top	732.00	3979.80	10	9/28/90
8A	0800 area	740.23	3976.38	45	10/1/89

† AT1 and AT2 were separate towers in close proximity.

‡ The UTM coordinates for site SR refer to zone 16, although this site is actually in zone 17.

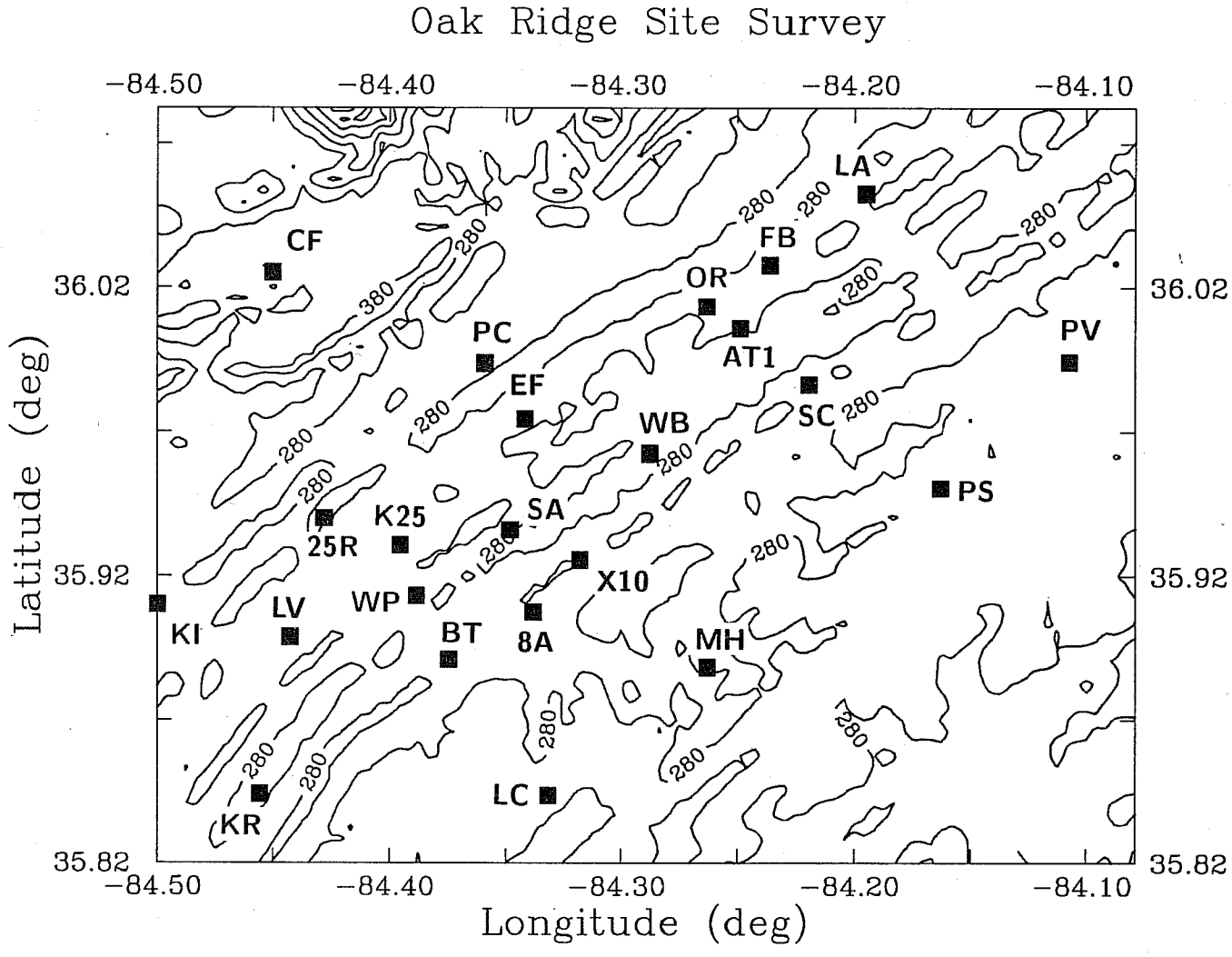

Fig. 4. Contour map of the Oak Ridge area showing the locations of the site-survey towers. The contours are in 100 m intervals.

release their measurements. The ASCOT data may be especially useful in regard to the wind flow through gaps in the 100 m ridges.

4. GENERAL WIND OBSERVATIONS

All but one of the sites in Table 3 can be placed into three terrain categories: Cumberland Mountain sites, ridge-top sites, and valley-bottom sites. Eight of the sites listed in the table are ridge-top sites, 17 are valley-bottom sites, and two are Cumberland Mountain sites. Site X10 is the one exception; it is located in a gap through one of the 100 m ridges. The three terrain categories are exposed to different terrain effects and sometimes to different wind regimes. General characteristics of the wind flow at these three site categories are discussed in this section.

As an example of the spatial variability that is present in the Oak Ridge area, Figs. 5–7 show the variations of temperature, wind speed, and wind direction at three site-survey towers during a five-day period in March 1990. Site BU is a Cumberland Mountain site, site WB is a ridge-top site, and site SC is a valley-bottom site. One-hour averages were used to create these figures.

Figure 5 indicates that cloudy skies prevailed until Julian day 62. Thereafter, a clear diurnal temperature cycle developed. As is expected, site BU had the smallest diurnal temperature variation, site SC the largest. During the night of Julian days 63–64, site BU did not show the nocturnal cooling evident at the other sites; this could be due to mountain-top clouds or warm-air advection at the level of BU. In general the temperature curves at sites WB and SC look similar, although the diurnal variation was greater at site SC. But during the night of Julian days 62–63, a warming event seems to have occurred at SC but not at WB. Another difference between these two sites occurred on day 64, when the nocturnal cooling proceeded much more rapidly at SC.

Figure 6 indicates that the variation of wind speed was quite different at the three sites. Site BU had a wind-speed maximum early on day 61 that corresponded to wind-speed minima at the other sites. The maximum at BU on day 62 also appeared at SC, but not at WB. At midnight on day 64, BU and WB had moderate winds, while SC was nearly calm. Day 64 at SC was fairly typical of the wind-speed variation observed on clear days at valley-bottom sites; nocturnal winds were nearly calm, whereas diurnal winds were typically around $2\,\mathrm{m\,s^{-1}}$. The other sites did not have this characteristic variation on day 64.

Figure 7 shows the variation of wind direction at the three sites. The most notable difference between the sites was the preponderance of northeasterly winds at sites WB and SC compared with site BU. On days 60 and 61, the northeasterly winds at the two lower sites were frequently opposite to the winds at BU. When the winds were not northeasterly, SC and to a lesser extent WB had a preference for southwesterly winds.

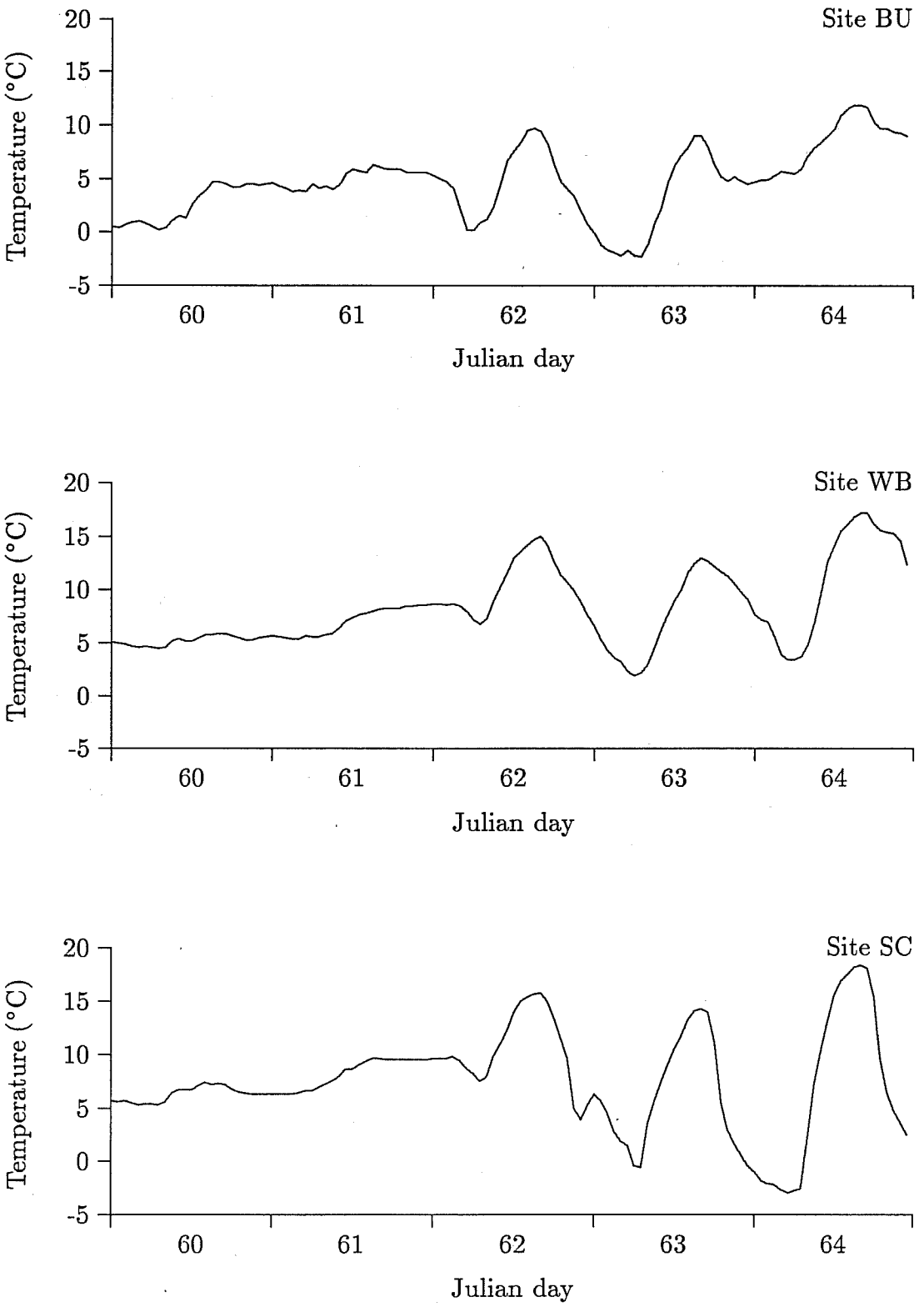

Fig. 5. Temporal variation of the one-hour-average temperature at sites BU (Cumberland Mountain), WB (ridge top), and SC (valley bottom). The plots cover the period from 1 to 5 March 1990.

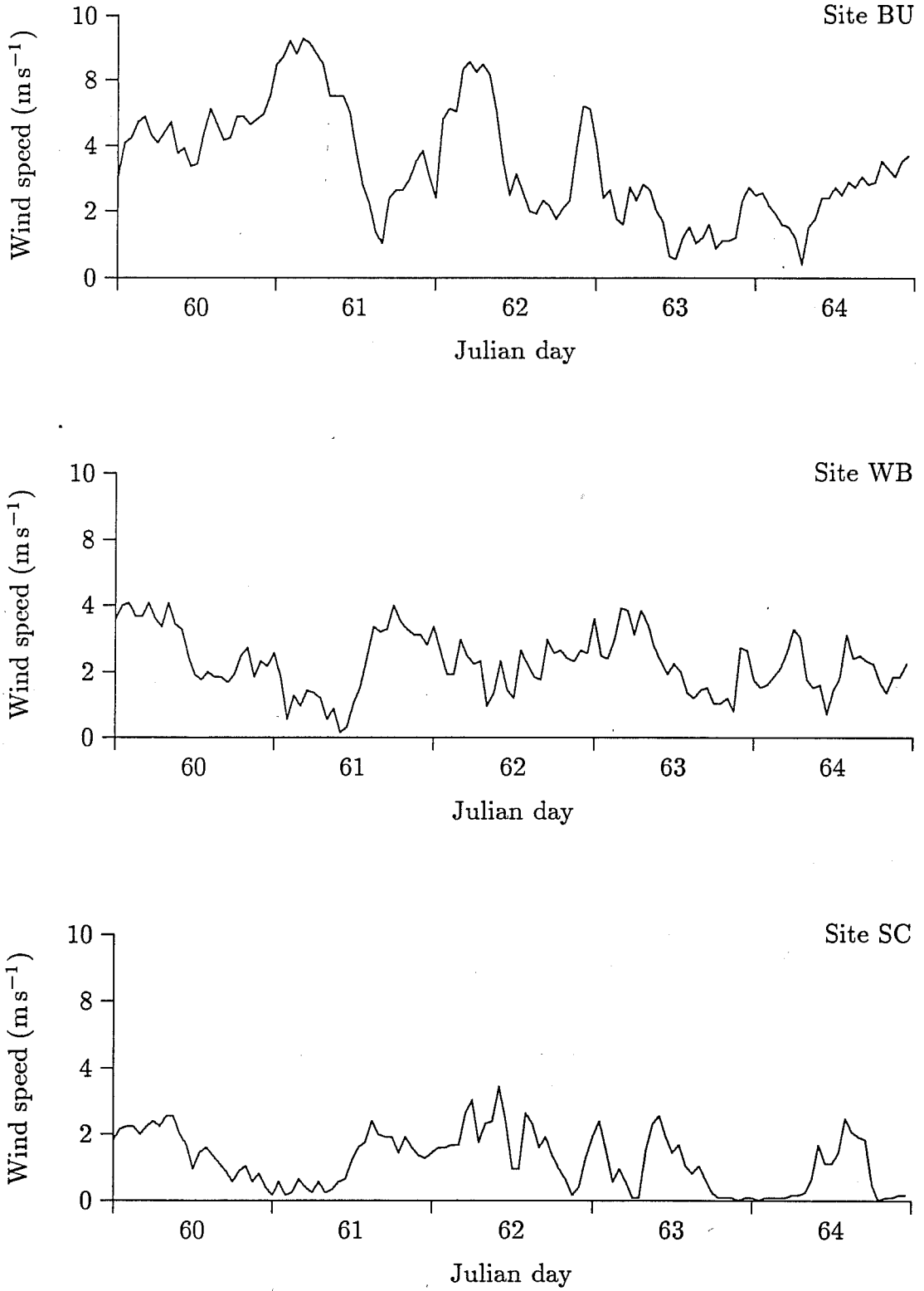

Fig. 6. Temporal variation of the one-hour-average wind speed at sites BU (Cumberland Mountain), WB (ridge top), and SC (valley bottom). The plots cover a five-day period from 1 to 5 March 1990.

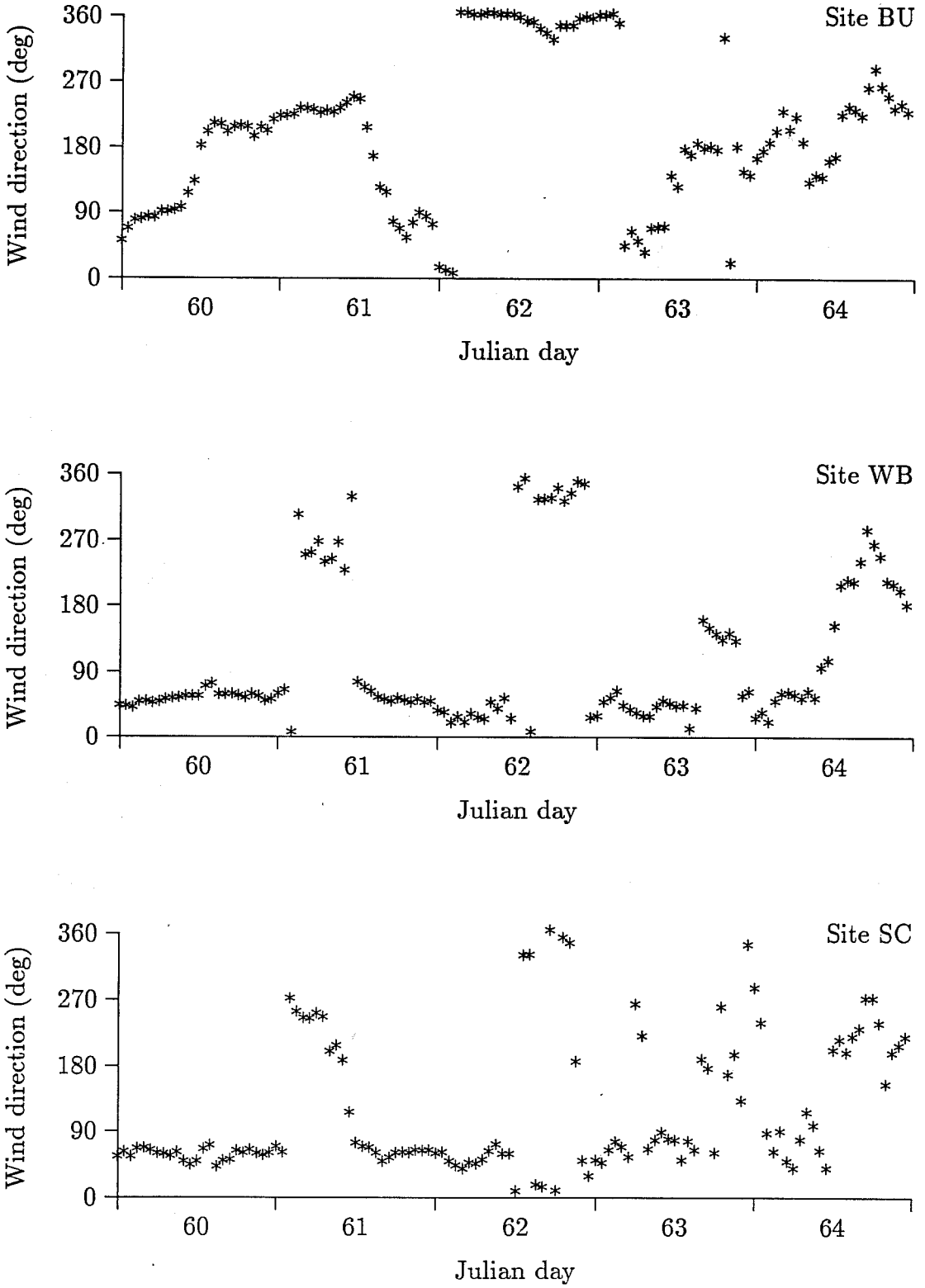

Fig. 7. Temporal variation of the one-hour-average wind direction at sites BU (Cumberland Mountain), WB (ridge top), and SC (valley bottom). The plots cover a five-day period from 1 to 5 March 1990.

This preference for northeasterly and southwesterly winds within the Tennessee River Valley has been noted in earlier studies (U.S. Weather Bureau, 1953; Nappo, 1977), and is most likely associated with the alignment of both the Tennessee River Valley and the smaller ridges within the valley. The channeling effect of the terrain also made the winds at WB and SC shift abruptly from one direction to another, whereas at BU the wind direction shifted more smoothly.

The figures presented so far in this section provide just one example of the wind variability exhibited in the Oak Ridge area. A statistically more meaningful approach to expressing the wind variability is to compute wind roses for various sites. In Fig. 8, one year of 15-minute-average data from selected sites has been used to produce eight-point wind roses, arranged by terrain category. Numbers in the center of the roses are the percentage of time the stations had 15-minute-average wind speeds less than $0.5\,\mathrm{m\,s^{-1}}$. The thin line along each direction represents the percentage of time the wind from that direction was between 0.5 and $5\,\mathrm{m\,s^{-1}}$. Speeds greater than $5\,\mathrm{m\,s^{-1}}$ are represented by small rectangles.

The most notable feature of the Cumberland Mountain wind roses in Fig. 8 is the rarity of easterly wind components. Site FH had a large southerly frequency that did not appear at site BU. This was probably the result of local terrain channeling. In general, the two Cumberland Mountain wind roses resemble those from stations in middle Tennessee (*e.g.*, Nashville), a pattern that reflects the overall synoptic flow in Tennessee (U.S. Weather Bureau, 1953).

Wind roses from the ridge-top sites indicate a channeling effect resulting from the southwest-northeast orientation of the Tennessee River Valley. Southeasterly winds were especially infrequent. Northeasterly winds were frequent but relatively light, suggesting the presence of nocturnal drainage flows in the Tennessee River Valley. At all the ridge-top sites, wind speeds of less than $0.5\,\mathrm{m\,s^{-1}}$ occurred less than 5% of the time. Three of the four ridge-top wind roses are also notable in having modes in the northwesterly or northerly directions. This may reflect the strong northwesterly or northerly winds that often follow cold front passages. Such wind directions were also frequent at the Cumberland Mountain sites.

Except for site X10, the valley-bottom wind roses in Fig. 8 strongly show a southwest-northeast channeling effect resulting from both the Tennessee River Valley and the smaller-scale ridges. The northwesterly mode seen at the higher sites was suppressed at the valley bottoms. At sites AT1 and OR, which are within the city of Oak Ridge, the winds were channeled into an east-west alignment. This different alignment may have resulted from much of the city being located within a gap in the 100 m ridges; both these sites have obstructing ridges to the southwest. Most of the valley-bottom sites in Fig. 8 had light winds ($< 0.5\,\mathrm{m\,s^{-1}}$) for 20% or more of the time. The exceptions were sites FB and OR, which may reflect the greater height of the instrument sets above the local surface (see Table 3).

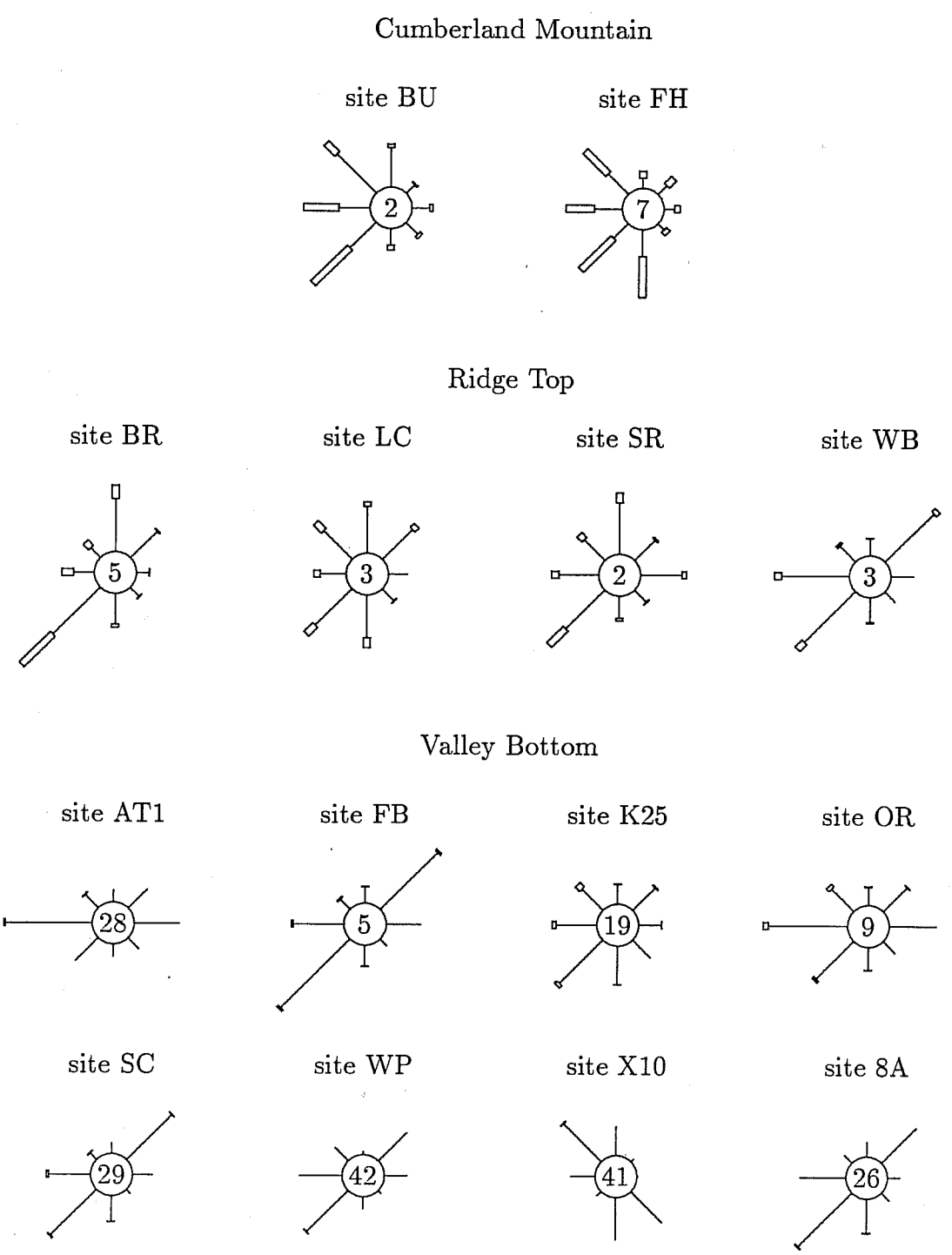

Fig. 8. Wind roses for selected sites in the Oak Ridge network. One year of 15-minute-average data was used for each wind rose. The central number represents the frequency (in percent) of wind speeds less than $0.5\,\mathrm{m\,s^{-1}}$. Thin lines along each direction represent the frequency of speeds between 0.5 and $5\,\mathrm{m\,s^{-1}}$. Speeds greater than $5\,\mathrm{m\,s^{-1}}$ are represented by small rectangles.

The peculiar wind rose for site X10 is a result of its location in a narrow gap. Winds within this gap were usually perpendicular to the winds in the valleys between the 100 m ridges. Site X10 also had a high frequency of light winds.

One of the complicating factors for simulating diffusion in the Oak Ridge area is the high frequency of light winds. Standard modeling techniques, such as the Gaussian plume model (see Hanna *et al.*, 1982), do not work well in calm conditions. To illustrate the predominance of light winds in the Oak Ridge area, cumulative frequency distributions of wind speed are presented in Fig. 9 for sites BU (Cumberland Mountain), WB (ridge top), and SC (valley bottom). These plots were derived from one year of 15-minute-average data. Site BU was obviously the windiest, with speeds less than $5\,\mathrm{m\,s^{-1}}$ approximately 65% of the time. At the other sites, wind speeds less than $5\,\mathrm{m\,s^{-1}}$ occurred more than 90% of the time. Wind speeds less than $2\,\mathrm{m\,s^{-1}}$ occurred about 70% of the time at SC. The wind speed frequency distributions seem to follow the commonly used Weibull distribution fairly well.

5. SPATIAL VARIABILITY OF THE HORIZONTAL WIND COMPONENTS

When modeling the transport of atmospheric contaminants, one always faces the problem of estimating the spatial wind field from a finite number of point measurements. The traditional and least expensive approach to this problem has been to employ a horizontally uniform wind field based on a single point measurement. In an area of complex terrain such as Oak Ridge, such a uniform wind field is clearly unrealistic over all but very short distances from the measurement site. But if a single measurement site is not adequate, then how many sites are adequate? How far apart should these sites be? How should the measurements be used to estimate the winds at other locations? No definitive answers are currently available for these questions. The answers depend in part on terrain complexity, the size of the region of interest, atmospheric conditions, and the averaging time used for the wind measurements.

In this section we focus on determining how far apart measurement sites should be in the Oak Ridge area to provide an adequate representation of the regional wind field. Both too large and too small site separations should be avoided. If the measurement sites are widely scattered, there is a risk that major features in the real wind field will go undetected. In contrast, densely packed sites can lead to redundant measurements and logistical problems in maintaining a large number of towers. Here, we address the problem of optimum site separation by looking at spatial variations in the wind measurements from the Oak Ridge site survey. A geostatistical tool called a variogram, briefly described in the following subsection, is used in this analysis.

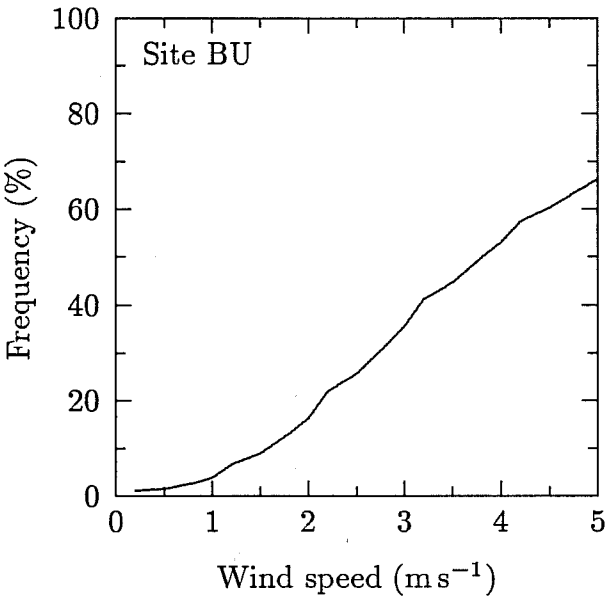

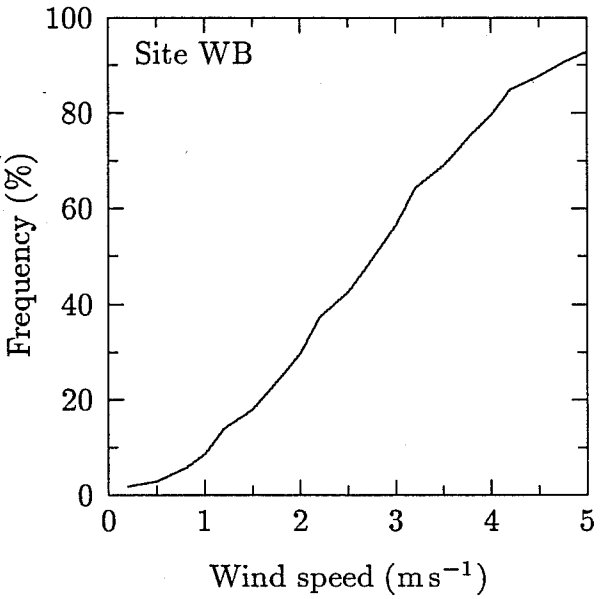

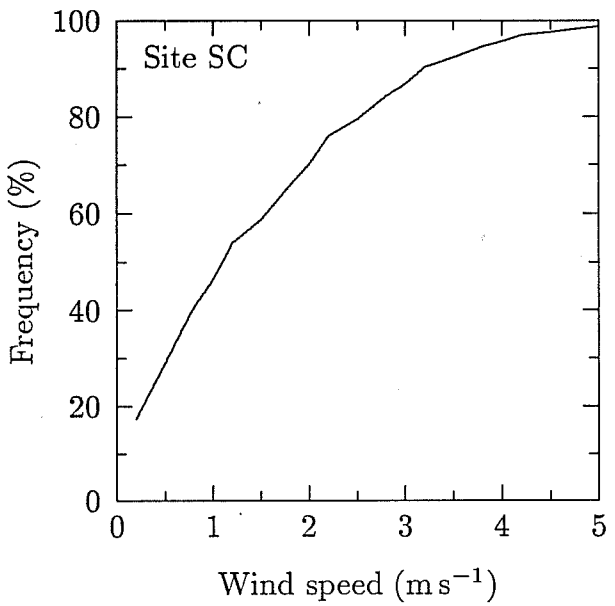

Fig. 9. Cumulative frequency distributions of the 15-minute-average wind speed for sites BU (Cumberland Mountain), WB (ridge top) and SC (valley bottom). One year of data was used to create each plot.

5.1. Overview of Variograms

The variogram is a graphical tool that is frequently used in geostatistics (see Journel and Huijbregts, 1978; Isaaks and Srivastava, 1989) to study spatial variability and as an initial step in the estimation method called kriging. It is similar to the correlogram, which is often used in turbulence studies. A correlogram is obtained by plotting the autocorrelation coefficient of a variable as a function of spatial or temporal separation. The variogram differs from the correlogram only by using the structure function instead of the autocorrelation coefficient.

Suppose a horizontal wind component u is sampled at two sites having locations designated by the position vectors $\mathbf{x}$ and $\mathbf{x} + \mathbf{d}$. If n samples are collected at each site, the two sets of wind measurements can be denoted by $u(\mathbf{x}, t_i)$ and $u(\mathbf{x} + \mathbf{d}, t_i)$, where t_i $(i = 1, 2, \ldots, n)$ represents the time at which one of the n samples was taken. The correlation coefficient is one parameter that can be used to study the relation between the measurements at the two sites. But the statistical parameter that has traditionally been used in geostatistics is one-half the structure function:

$$\gamma(\mathbf{x}, \mathbf{d}) = \frac{1}{2n} \sum_{i=1}^{n} \left[u(\mathbf{x} + \mathbf{d}, t_i) - u(\mathbf{x}, t_i)\right]^2$$

$$= \frac{1}{2} \overline{\left[u(\mathbf{x} + \mathbf{d}, t_i) - u(\mathbf{x}, t_i)\right]^2} \,. \qquad (1)$$

The overbar denotes averaging over the n samples. When there is little difference between the winds at the two sites, γ approaches zero; when the winds significantly differ, γ approaches the average of $\overline{u^2(\mathbf{x}, t_i)}$ and $\overline{u^2(\mathbf{x} + \mathbf{d}, t_i)}$.

A variogram is formed from measurements at several pairs of sites by plotting γ on the ordinate and separation on the abscissa. The separation can be either a component of $\mathbf{d}$ or its magnitude d. In the latter case the resulting graph is called an omnidirectional variogram.

Although γ in general depends on both $\mathbf{x}$ and $\mathbf{d}$, only the variation with $\mathbf{d}$ is considered in a variogram. In complex terrain such as the Oak Ridge area, the variability of γ with $\mathbf{x}$ can be significant. One effect of the $\mathbf{x}$ dependence is to produce scatter in the variogram, since different site pairs have different values of $\mathbf{x}$. If this scatter is large enough, the variation of γ with separation may be difficult to observe.

Variograms typically have a shape resembling that indicated in Fig. 10. Up to a point, γ tends to increase with increasing separation because the measurements at two sites tend to become less correlated as the separation between the sites increases. At larger separations the variogram forms a plateau. Measured variograms also tend to show a discontinuity when they are extrapolated to zero separation, because some spatial variability is present at scales that are too small to be resolved in the

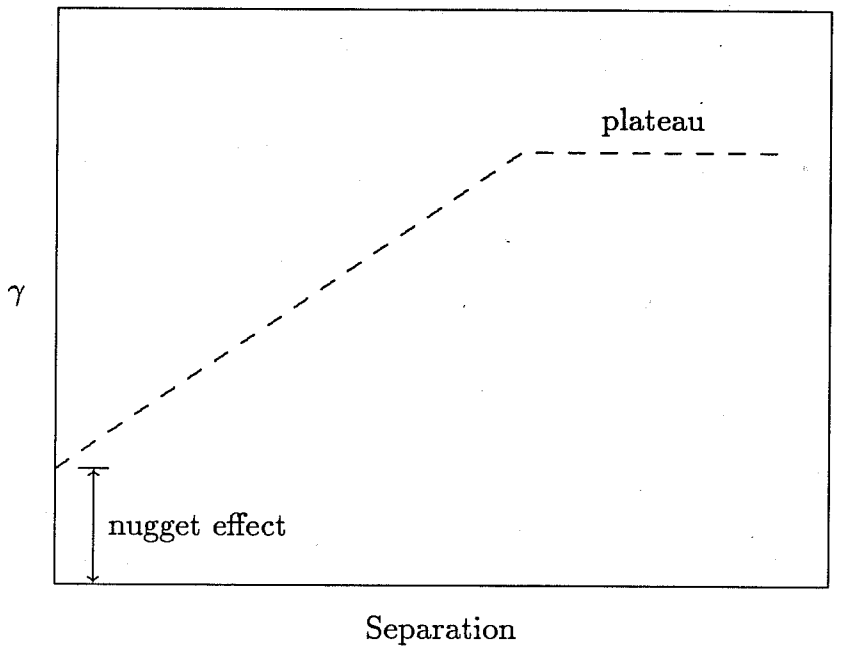

Fig. 10. Schematic illustration of a variogram having a plateau at large separations. For simplicity, linear variations of γ are shown, although real variograms can have nonlinear variations of γ.

measurements. In geostatistics this discontinuity is usually called the nugget effect (which alludes to the roots of geostatistics in mining studies).

We chose to use the variogram in our analysis because the statistic γ accounts for spatial variations in both the sample mean $\overline{u}$ and the fluctuations $u' = u - \overline{u}$. In contrast, the autocorrelation coefficient accounts only for variations in u'. For contaminant transport, the spatial variations of both $\overline{u}$ and u' are of interest, so γ provides a more complete picture than the correlation coefficient.

One problem with the statistic γ is its dimensionality. The variograms would be easier to interpret and compare if a dimensionless form of γ is defined. Additionally, a normalized γ may have less scatter resulting from the dependence on $\mathbf{x}$. Several normalized versions of γ have been suggested (see Isaaks and Srivastava, 1989, pp. 163–170), but there is no consensus on which form is the best. Variograms which use a normalized γ are called relative variograms.

For our analysis we use the following normalized γ:

$$\gamma_r(\mathbf{x}, \mathbf{d}) = \frac{2\gamma(\mathbf{x}, \mathbf{d})}{\overline{u^2(\mathbf{x}, t_i)} + \overline{u^2(\mathbf{x} + \mathbf{d}, t_i)}} . \tag{2}$$

This statistic can be interpreted as the ratio of the mean-square difference of u at the

two sites to the mean-square magnitude of u. It approaches zero when the values of u at the two measurement sites are in close agreement and approaches unity when the difference between the values of u at the sites is about the same size as the magnitude of u. If the values of u at the two sites tend to have opposite signs, γ_r can fall in the range from 1 to 2. The statistic γ_r seems to produce less scatter in the Oak Ridge wind data than some of the other relative variograms suggested by Isaaks and Srivastava (1989). In the following section, γ_r is used to create omnidirectional variograms for the Oak Ridge site-survey data.

5.2. Omnidirectional Variograms for the Oak Ridge Data

The 15-minute-average wind data from the Oak Ridge site survey were chosen for the variogram analysis. These data are more representative of the transport winds used in a dispersion model than are the one-minute data. Since the terrain has a distinct southwest-northeast alignment, we rotated the horizontal coordinate system so the positive x axis points towards 52°. The variables u and v respectively denote the along-valley and cross-valley wind components.

Three weeks of site-survey data from November 1990 were chosen for computing the relative variograms. This month was chosen because most of the sites in Table 3 were fully operational. The winds in Oak Ridge are somewhat stronger during November than during some other times of the year (U.S. Weather Bureau, 1953), so our analysis may not reflect, for example, the wind flow during the summer months, when light winds prevail.

Not all the sites in Table 3 were included in the variogram analysis. The two Cumberland Mountain sites (BU and FH) are in a significantly different flow regime from all the other sites and were thus excluded. Site CF was likewise omitted because of its proximity to the Cumberland Mountains. Site X10 is located in a gap through one of the 100 m ridges, so it was excluded. The breeder site BT was not used because the raw data from this site had not been processed in time for the analysis. Site AT2 had already been dismantled by November 1990. With these exclusions, 22 sites remain. Fourteen of these sites are in valley bottoms, and eight are on ridge tops.

Separate variograms were constructed for the ridge-top and valley-bottom sites. The data were stratified into three wind-speed categories: 0.5–2 $\mathrm{m\,s^{-1}}$, 2–5 $\mathrm{m\,s^{-1}}$, and greater than 5 $\mathrm{m\,s^{-1}}$. A wind-speed stratification was used because other studies (*e.g.*, Ross and Smith, 1986) indicate that the correlation between measurement sites decreases as wind speed decreases. In the valley bottoms, the proper speed category for a particular 15-minute period was determined by averaging the wind-speed measurements at all the valley-bottom sites. Similarly, the proper ridge-top speed category was determined by averaging the speed measurements at all the ridge-top sites. Speeds of less than 0.5 $\mathrm{m\,s^{-1}}$ were not considered, because this is near the threshold of the propeller anemometers.

Figures 11 and 12 are the valley-bottom variograms for the 0.5–2 m s^{-1} and 2–5 m s^{-1} speed categories. (The available data were insufficient to produce valley-bottom variograms for the > 5 m s^{-1} category.) These variograms show evidence of a downturn at small separations. Plateaus are reached in the along-valley variograms at separations of about 7–8 km in Fig. 11 and 10 km in Fig. 12. For the cross-valley component, plateaus are reached at approximately 5 km in both figures. The values of γ_r at the plateaus in Fig. 11 are 0.5–0.6 for the u component and 0.8 for the v component. For Fig. 12, the corresponding values are 0.2 and 0.4. These plateaus are reached when γ_r is less than unity, because mesoscale and synoptic-scale atmospheric motions produce residual correlations between the measurement sites.

Figure 13 shows the ridge-top variograms for the 0.5–2 m s^{-1} speed category. Both the along-valley and cross-valley plots reach plateaus at separations of about 12–13 km. The values of γ_r at the plateaus are also similar, being about 0.6 for the u component and 0.65 for the v component. The similarity between the u and v variograms in Fig. 13 contrasts with the differences between the components observed in the valley-bottom variograms.

The ridge-top variograms for the 2–5 m s^{-1} and > 5 m s^{-1} speed categories are shown in Figs. 14 and 15. All the variograms except for the u component in Fig. 15 reach plateaus at separations of about 15 km. The plateaus for the cross-valley component are at $\gamma_r = 0.4$ in Fig. 14 and $\gamma_r = 0.25$ in Fig. 15. For the along-valley component, the plateaus are more difficult to evaluate, because the variograms start to increase again at separations beyond about 35 km. The temporary plateaus extending from 15 to 35 km have values of 0.25 in Fig. 14 and 0.12 in Fig. 15. The increase in γ_r beyond 35 km may indicate the presence of atmospheric motions having scales on the order of 40–50 km at ridge-top level.

In regard to the representativeness of wind measurements, the variograms can be used to define "areas of influence" (Cressman, 1959; Goodin *et al.*, 1979) for the measurement sites. Each measurement site is assumed to be representative of the winds within its own area of influence. To be effective, the areas of influence produced by a network of measurement sites should cover a significant fraction of the total region of interest. Otherwise, the network may fail to detect significant features in the wind field. In an ideal situation, the measurement sites would have abutting areas of influence.

The size of a measurement's area of influence partly depends on the specific problem that is being addressed. For example, the areas of influence appropriate for microscale pollutant transport would be significantly smaller than those appropriate for mesoscale transport. This degree of arbitrariness in defining areas of influence is somewhat analogous to the problem of determining an appropriate level of confidence in statistical analysis; for some problems a 90% confidence level is sufficient, whereas for others a higher level of confidence is required. The size of an area of influence also depends on the averaging time used for the wind measurements. An averaging time of one minute will produce smaller areas of influence than a 15-minute averaging time.

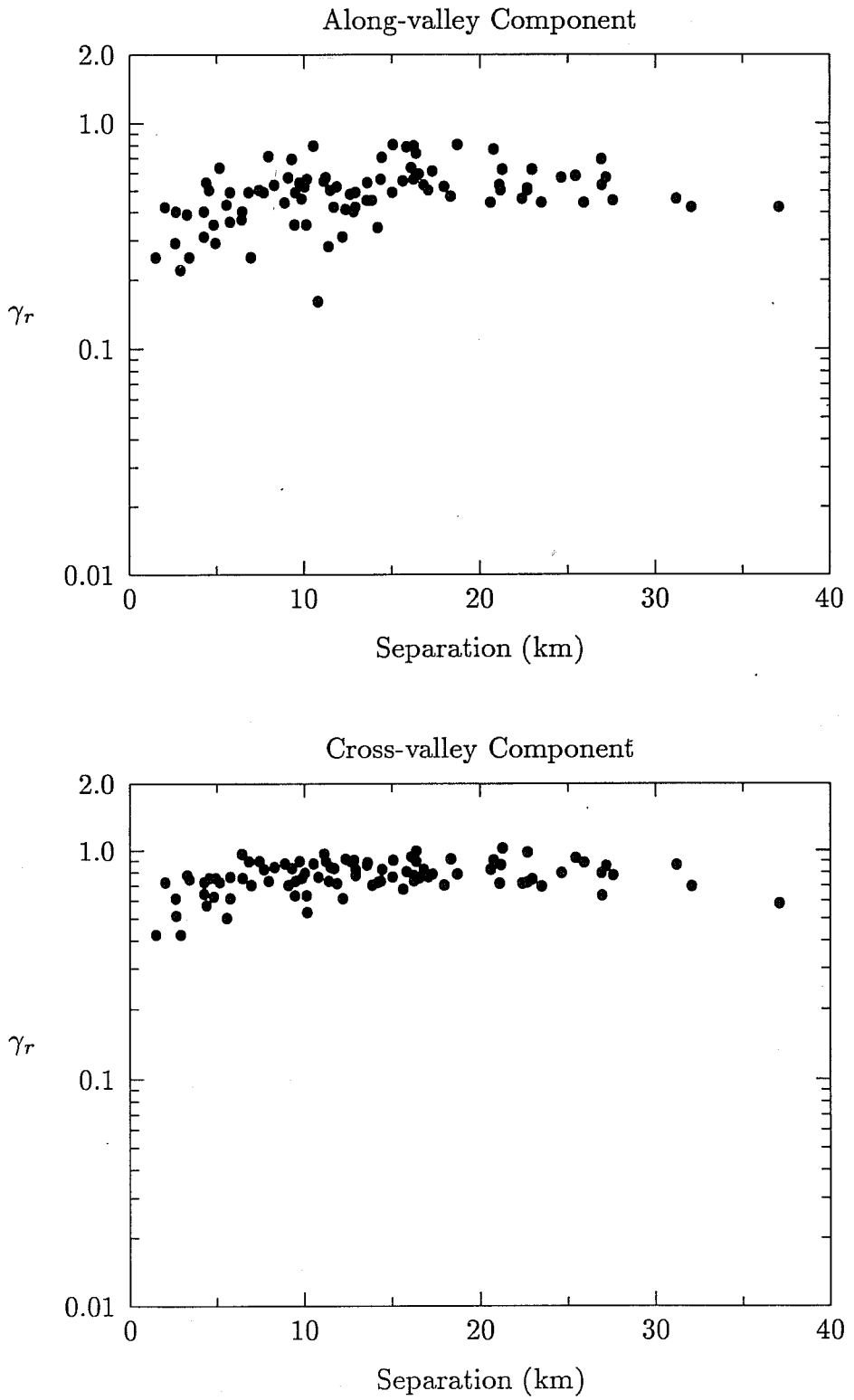

Fig. 11. Omnidirectional variograms for the valley-bottom sites when the 15-minute-average wind speed was between 0.5 and 2 m s^{-1}. The upper plot shows the along-valley wind component, and the lower plot shows the cross-valley component.

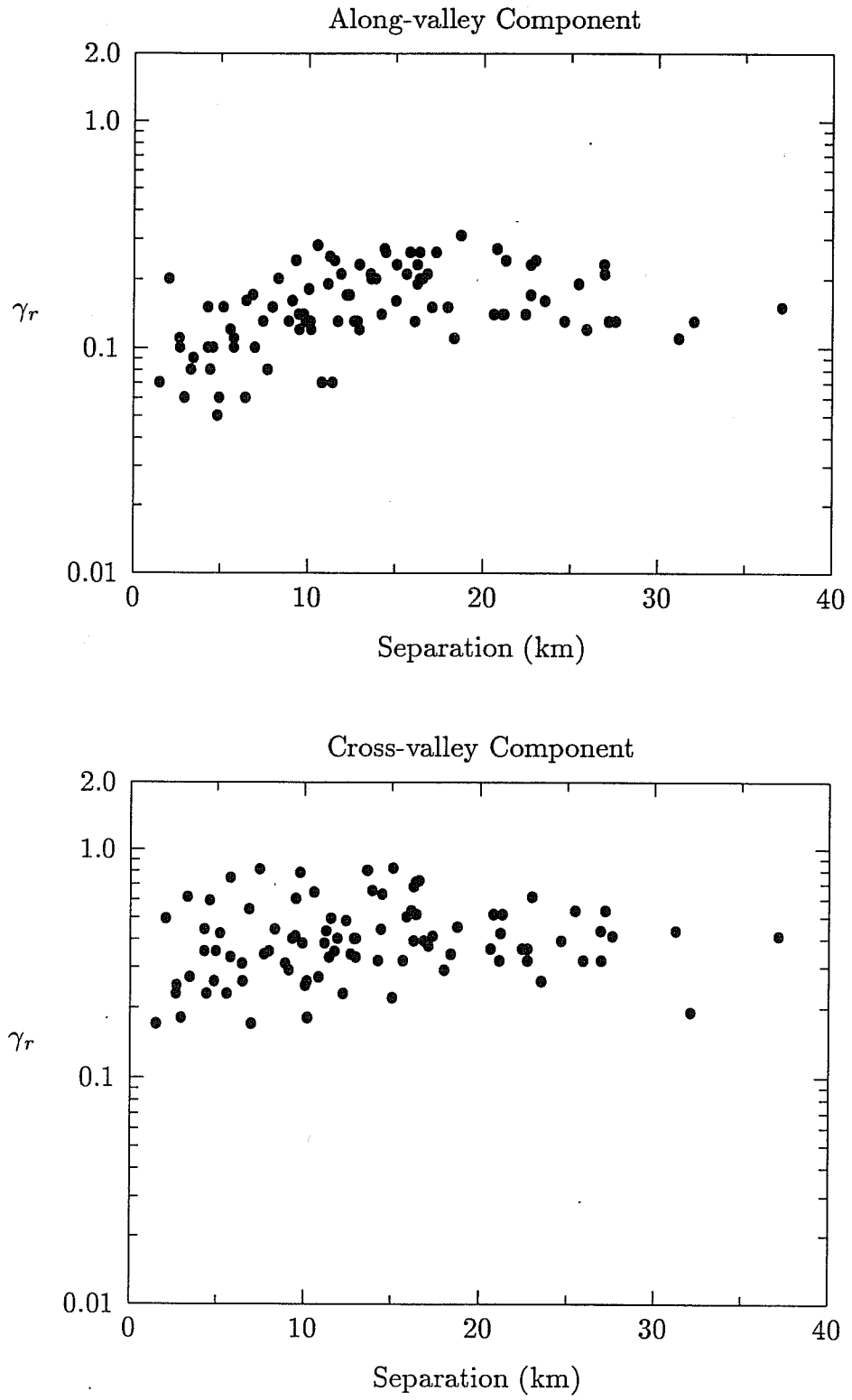

Fig. 12. Omnidirectional variograms for the valley-bottom sites when the 15-minute-average wind speed was between 2 and 5 $\mathrm{m\,s^{-1}}$. The upper plot shows the along-valley component, and the lower plot shows the cross-valley component.

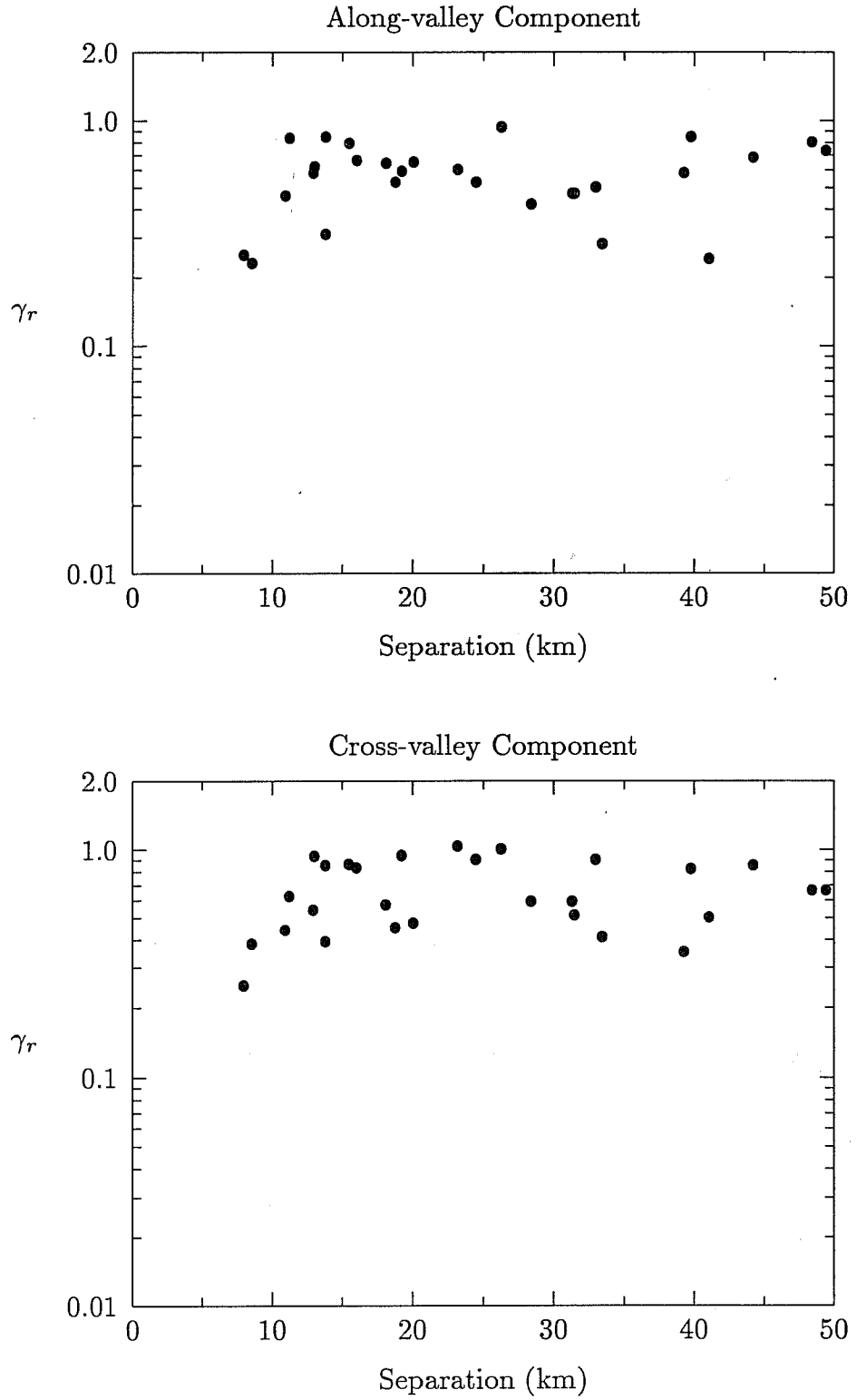

Fig. 13. Omnidirectional variograms for the ridge-top sites when the 15-minute-average wind speed was between 0.5 and $2\,\mathrm{m\,s^{-1}}$. The upper plot shows the along-valley wind component, and the lower plot shows the cross-valley component.

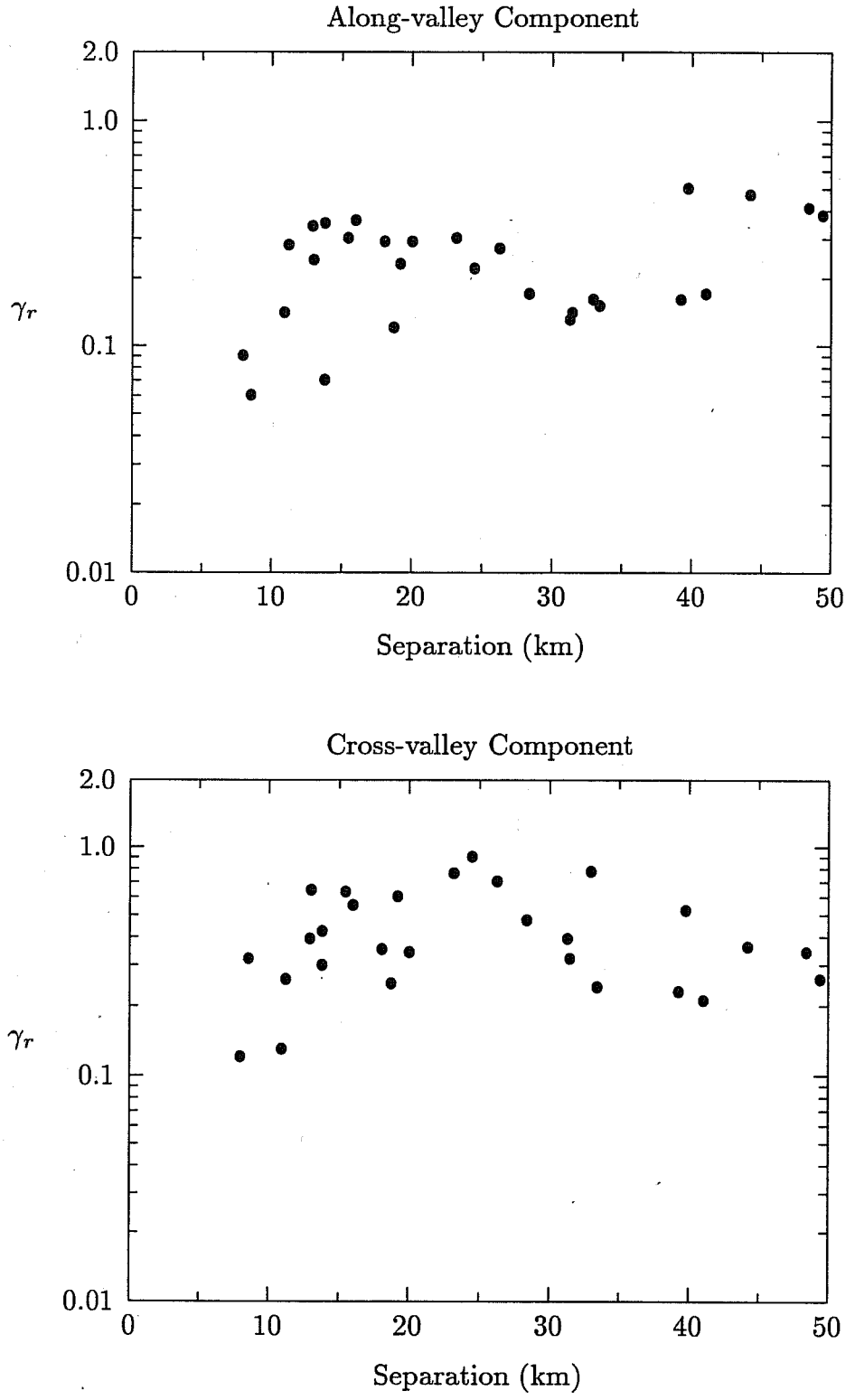

Fig. 14. Omnidirectional variograms for the ridge-top sites when the 15-minute-average wind speed was between 2 and 5 $\mathrm{m\,s^{-1}}$. The upper plot shows the along-valley wind component, and the lower plot shows the cross-valley component.

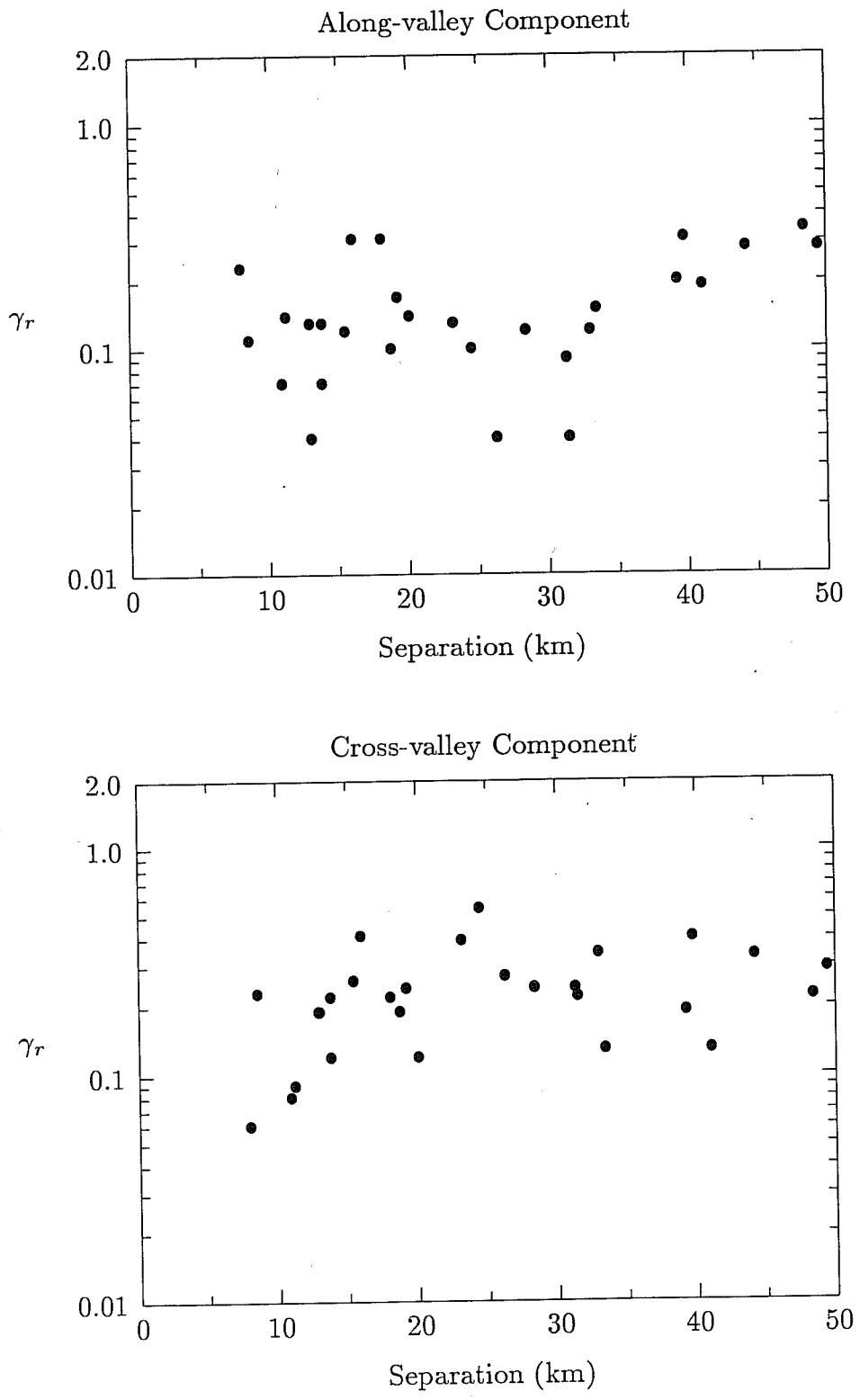

Fig. 15. Omnidirectional variograms for the ridge-top sites when the 15-minute-average wind speed was greater than $5\,\mathrm{m\,s^{-1}}$. The upper plot shows the along-valley wind component, and the lower plot shows the cross-valley component.

In interpreting the Oak Ridge variograms, we assume that the areas of influence for the measurement sites are roughly circular. The radii of these areas can be defined as the separation at which some critical value of γ_r is first reached in a variogram. We chose to use $\gamma_r = 0.25$ as the critical value. At this value, Eq. (2) indicates that the root-mean-square difference of u at the two sites is about 50% of the root-mean-square magnitude of u.

Table 4 shows the radii of influence obtained from the Oak Ridge variograms using $\gamma_r = 0.25$ as the critical value. In the valley bottoms, the radius of influence for the u measurements is approximately 3–4 km for the lowest speed category and is greater than the maximum available separation for the 2–5 m s^{-1} category. The valley-bottom v measurements have a radius of influence that is less than the minimum available separation for the 0.5–2 m s^{-1} speed category and is about 5 km for the 2–5 m s^{-1} category. At ridge top, the u radius of influence ranges from 9 to about 40 km, whereas the v radius of influence ranges from 8 to about 20 km.

As was mentioned previously, a network of measurement sites should have abutting areas of influence to minimize the risk of missing important features in the wind field. The individual measurement sites would then have average separations equal to twice the radius of influence. For the Oak Ridge area, this criterion means the separations between the valley-bottom sites should be no more than approximately 6–8 km (see Table 4) to provide adequate coverage of the along-valley wind component. The radius of influence for the valley-bottom v component is so small for the 0.5–2 m s^{-1} speed category that it would be impractical to install a sufficient number of towers. At higher wind speeds, an average separation of no more than 10 km would be adequate for this component. The ridge-top sites should have separations of no more than 16–18 km to provide adequate coverage in all the speed categories.

Table 4. Estimated radii of influence for the Oak Ridge measurement sites. The estimates were obtained from the Oak Ridge variograms using $\gamma_r = 0.25$ as the critical value

Wind speed (m s^{-1})	Valley-bottom sites		Ridge-top sites	
	u radius (km)	v radius (km)	u radius (km)	v radius (km)
0.5–2	3–4	†	9	8
2–5	> 40	5	15	13
>5	‡	‡	42	21

† Radius is less than minimum separation.

‡ Variograms were not available for this speed category.

The site separations suggested by the variogram analysis are affected by the choice of a critical value for γ_r. In addition, a considerable amount of scatter makes some of the variograms difficult to interpret. Hence, the site separations suggested by Table 4 should be interpreted as rough estimates, and not as precise measurements.

6. INTERPOLATION OF THE OAK RIDGE WIND FIELD

In the foregoing section, some of the problems associated with modeling the Oak Ridge wind field were addressed by investigating the spatial variability of the site-survey wind data. In this section a different approach is employed to address these same problems. By assessing the performance of two interpolation models, we attempt to determine how many measurement sites are required in the Oak Ridge area to provide an adequate representation of the wind field. Presumably, adding more sites to a network eventually produces diminishing returns. When this point is reached, little additional information about the wind field is obtained by adding more measurement sites.

6.1. Description of Interpolation Models

One of the simplest interpolation techniques for wind-field modeling is $1/r^2$ interpolation (Wendell, 1972; Goodin *et al.*, 1979). In this technique, the interpolated wind components $\hat{u}(\mathbf{x}_j, t)$ and $\hat{v}(\mathbf{x}_j, t)$ at a location $\mathbf{x}_j$ and time t are obtained from observations at N other sites by the following weighted sums:

$$\hat{u}(\mathbf{x}_j, t) = \left(\sum_{i=1}^{N} u(\mathbf{x}_i, t)/r_{ij}^2 \right) \Bigg/ \left(\sum_{i=1}^{N} 1/r_{ij}^2 \right) ;$$

$$\hat{v}(\mathbf{x}_j, t) = \left(\sum_{i=1}^{N} v(\mathbf{x}_i, t)/r_{ij}^2 \right) \Bigg/ \left(\sum_{i=1}^{N} 1/r_{ij}^2 \right) . \qquad (3)$$

The variable r_{ij} is the distance between $\mathbf{x}_i$ and $\mathbf{x}_j$. In later discussions, Eq. (3) is called the simple $1/r^2$ model.

For $N = 1$, Eq. (3) produces a spatially uniform wind field. This is the wind field used in the Gaussian plume model for atmospheric diffusion (see Hanna *et al.*, 1982). When $N > 1$, the influence of a measurement in Eq. (3) is inversely proportional to the square of its distance from the point of interpolation. This distance weighting can be considered to be a rough approximation to the area-of-influence concept discussed in section 5.

One problem with the simple $1/r^2$ model is that it weights the observations only by their distance from the point of interpolation. It does not account for terrain differences

such as the ridge-top and valley-bottom sites in the Oak Ridge site survey. One possible improvement to the $1/r^2$ interpolation is to include an additional weighting factor a_{ij} that reflects terrain differences at the locations $\mathbf{x}_i$ and $\mathbf{x}_j$:

$$\hat{u}(\mathbf{x}_j,t) = \left(\sum_{i=1}^{N} a_{ij}u(\mathbf{x}_i,t)/r_{ij}^2\right) \Big/ \left(\sum_{i=1}^{N} a_{ij}/r_{ij}^2\right) ;$$
$$\hat{v}(\mathbf{x}_j,t) = \left(\sum_{i=1}^{N} a_{ij}v(\mathbf{x}_i,t)/r_{ij}^2\right) \Big/ \left(\sum_{i=1}^{N} a_{ij}/r_{ij}^2\right) . \tag{4}$$

Equation (4) is called the terrain-modified $1/r^2$ model in later discussions.

Table 5 is one possible set of terrain weighting factors that could be used in Oak Ridge. Sites that are in unusual terrain, such as site X10, fall into the "other" category. The weighting factors in Table 5 ensure that ridge-top measurements are primarily used to interpolate to other ridge-top locations, and valley-bottom measurements are primarily used to interpolate to other valley-bottom locations.

6.2. Interpolation of the Site-survey Wind Data

To assess the performance of the interpolation models described in section 6.1, some quantitative comparison must be made between the wind observations and the corresponding model estimates. No consensus has arisen regarding the most suitable statistics for evaluating model performance, so meteorologists have chosen various statistics (*e.g.*, Lanicci and Weber, 1986; Lange, 1989; Gou and Palutokof, 1990). Here, we use a version of the statistic γ_r defined in section 5:

$$\gamma_r(\mathbf{x}) = \frac{\overline{\left[\hat{u}(\mathbf{x},t) - u(\mathbf{x},t)\right]^2}}{\overline{\hat{u}^2(\mathbf{x},t)} + \overline{u^2(\mathbf{x},t)}} . \tag{5}$$

The variables $u(\mathbf{x},t)$ and $\hat{u}(\mathbf{x},t)$ respectively denote the observed and interpolated values of the wind component u at the location $\mathbf{x}$ and time t. A similar equation can be written for the cross-valley component v.

Table 5. Terrain weighting factors used to interpolate the horizontal wind components

	Interpolation site		
Observation site	Valley	Ridge	Other
Valley	1.0	0.0	0.5
Ridge	0.0	1.0	0.5
Other	0.5	0.5	0.5

We used γ_r to evaluate the performance of the interpolation models when different numbers N of observation sites are used as input. The three-week data set described in section 5 was used in the analysis. This data set contains 22 measurement sites, so the maximum value of N is 21; this leaves at least one measurement site for computing γ_r. The data were stratified into the same wind-speed categories that were used in section 5. Since the ridge-top and valley-bottom sites are both used in the interpolations, the proper speed category for each 15-minute period was determined by the average wind speed at the valley-bottom sites.

We evaluated the interpolation models using the following values of N: 1, 2, 4, 8, 16, and 21. Since there are 22 available observation sites, many different site combinations can be created for each value of N. It is impractical to investigate all these combinations. For example, there are 319,770 possible combinations of eight sites that can be obtained from the 22 that are available. Even if all the possible combinations could be investigated, many would be of little practical interest, because they are poorly distributed and do not contain reasonable proportions of ridge-top and valley-bottom sites. To limit the analysis, we chose ten different site combinations for each value of N. Each combination was intended to provide well distributed measurements both at the ridge tops and in the valley bottoms.

Once a particular combination of N sites was chosen, the November 1990 data for these towers were used as input to the interpolation models described in section 6.1. An estimate of the statistic γ_r in Eq. (5) was then computed for each of the $(22-N)$ remaining measurement sites. These $(22-N)$ estimates of γ_r were averaged to produce a single value $\overline{\gamma_r}$ that characterizes the model performance for the specific site combination. This process was repeated for all ten combinations of N sites. The ten values of $\overline{\gamma_r}$ were then averaged to produce a single estimate $\langle\gamma_r\rangle_N$ representing the model performance for N input sites. A 95% confidence interval for $\langle\gamma_r\rangle_N$ was estimated by assuming that it follows a t distribution with nine degrees of freedom. (*i.e.*, $\langle\gamma_r\rangle_N$ is a sample mean from a sample size of ten.)

Figure 16 shows how $\langle\gamma_r\rangle_N$ varies with the number of sites for the simple $1/r^2$ model. Vertical bars are used to indicate the estimated 95% confidence intervals for the data. For all values of N, the model's skill clearly worsens as the wind speed decreases. This is explained by the increasing dominance of small-scale flows as the speed decreases (see Table 4 and Ross and Smith, 1986).

As is expected, $\langle\gamma_r\rangle_N$ in Fig. 16 tends to decrease as the number of input sites increases. Except for the data points at $N = 21$, which have unusually large confidence intervals, the curves tend to become more horizontal at larger values of N. This suggests that beyond a certain value of N, the simple $1/r^2$ model gets diminishing returns from subsequent increases in the number of input sites.

Figure 17 shows the variation of $\langle\gamma_r\rangle_N$ for the terrain-modified $1/r^2$ model. The general shapes of the curves are similar to those in Fig. 16. But at larger values of N,

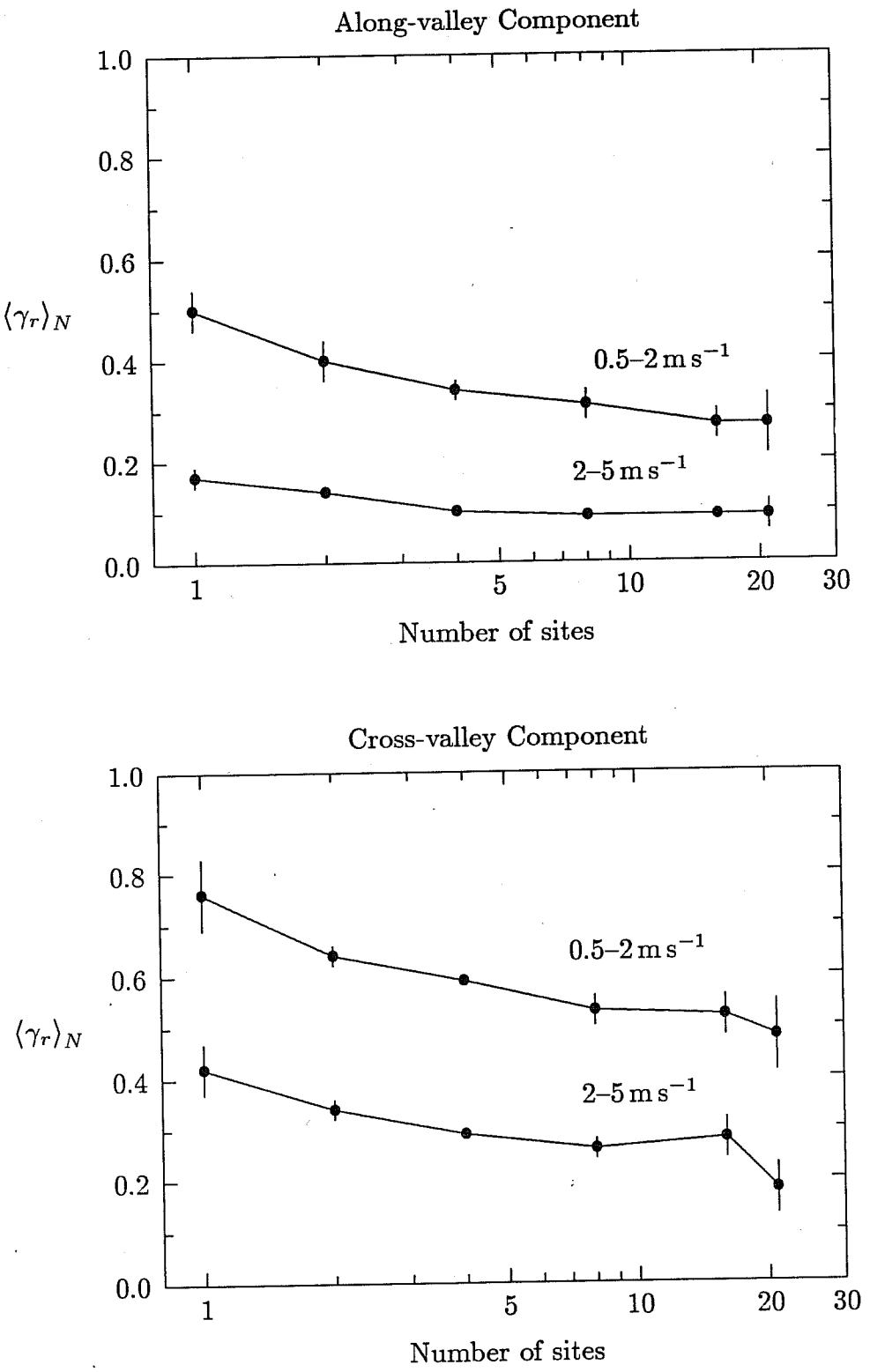

Fig. 16. Variation of $\langle \gamma_r \rangle_N$ with the number of input sites for the simple $1/r^2$ model. A separate curve is drawn for each wind-speed category. The vertical lines represent 95% confidence intervals for the data.

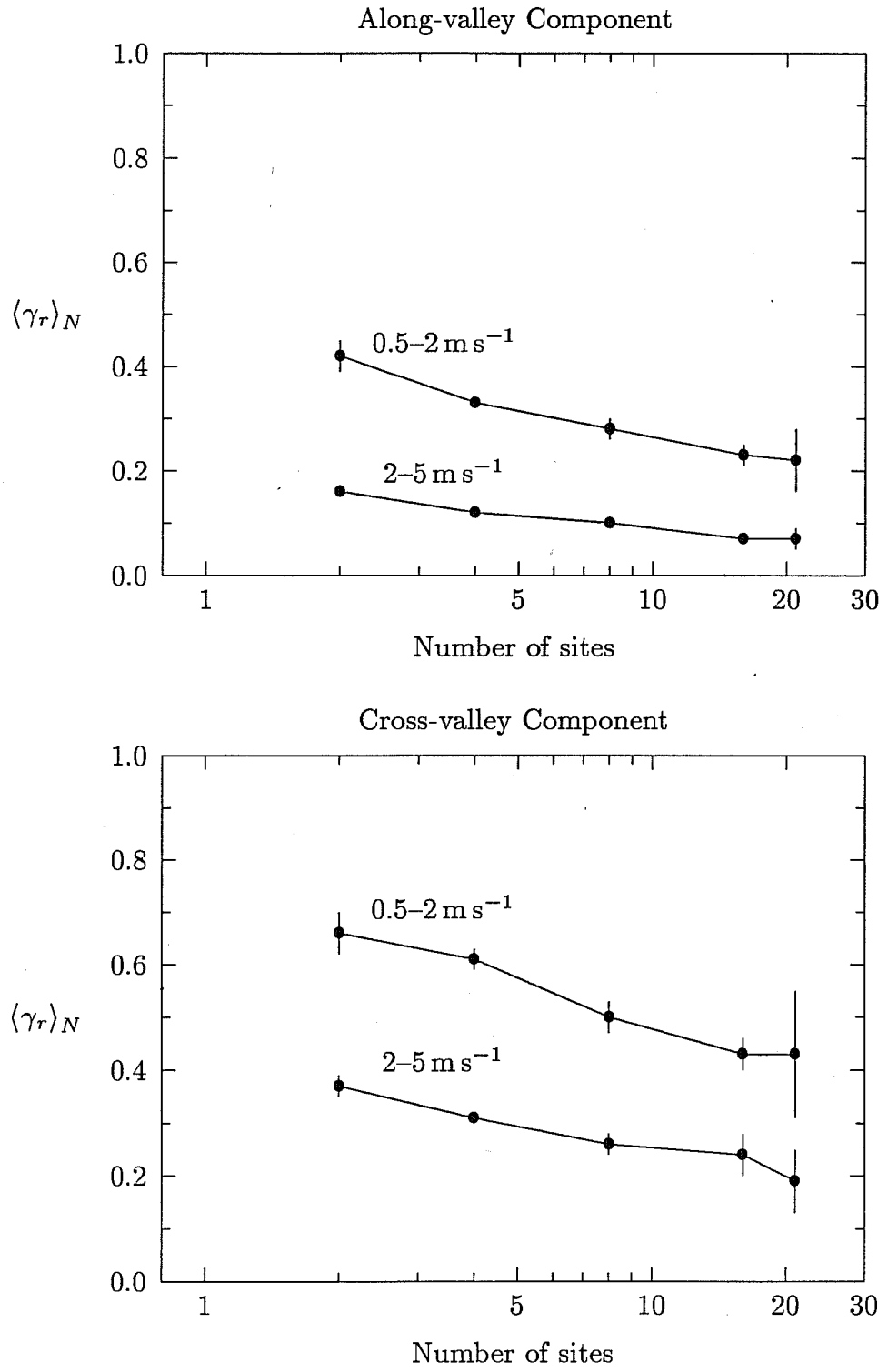

Fig. 17. Variation of $\langle \gamma_r \rangle_N$ with the number of input sites for the terrain-modified $1/r^2$ model. Separate curves are plotted for each wind-speed category. The vertical bars indicate 95% confidence intervals for the data.

the curves in Fig. 17 are somewhat steeper than they are in Fig. 16. Hence, the terrain-modified $1/r^2$ model seems to reach diminishing returns at larger values of N than the simple $1/r^2$ model. More generally, this result suggests that the optimum number of towers for the Oak Ridge area partly depends on which wind-field model is employed.

As is done in section 5, a critical value of $\langle \gamma_r \rangle_N$ can be used in Figs. 16 and 17 to estimate the minimum number of wind measurement sites required for the Oak Ridge area. Table 6 shows the results when 0.25 is used as the critical value of $\langle \gamma_r \rangle_N$. Both models give more or less the same results. The numbers in this table broadly agree with the variogram results in Table 4. For light winds, Table 6 indicates that an impractically large number of measurement sites would be required to adequately sample the cross-valley component; a similar conclusion is reached for the valley-bottom sites in Table 4. For stronger winds, both Table 6 and the valley-bottom results in Table 4 suggest that the along-valley component is highly uniform over the entire region, whereas the cross-valley component is still significantly affected by smaller-scale flows. The main reason Table 6 agrees with the valley-bottom results in Table 4 is that most of the measurement sites used in the interpolations are valley-bottom sites.

To evaluate the relative performance of the interpolation models for the along-valley and cross-valley wind components, the ratio of $\langle \gamma_r \rangle_N$ for the v component to $\langle \gamma_r \rangle_N$ for the u component is plotted in Fig. 18. The ratio always exceeds unity for both models, indicating that the models are better at estimating the along-valley wind component. There is also a consistent tendency for the ratio to be larger at higher wind speeds. One explanation for this tendency is that the higher winds may have been channeled into a southwest-northeast orientation by the local terrain. Hence, the along-valley component u was dominated by a large mean value that had relatively little spatial variability, whereas the cross-valley component v had a smaller mean value and was dominated by local perturbations in the wind field. Another feature of Fig. 18 is the tendency of the ratio to increase as the number of towers increases. Adding more measurement sites seems to improve the models' skill in estimating the along-valley component more than their skill in estimating the cross-valley component.

Table 6. Estimates of the minimum number of wind measurement sites required to adequately sample the regional wind field around Oak Ridge. The estimates were obtained from the simple and terrain-modified $1/r^2$ models using 0.25 as the critical value for $\langle \gamma_r \rangle_N$

Wind speed ($\mathrm{m\,s^{-1}}$)	Simple model		Terrain-modified model	
	u sites	v sites	u sites	v sites
0.5–2	16	>21	16	>21
2–5	1	8	2	8

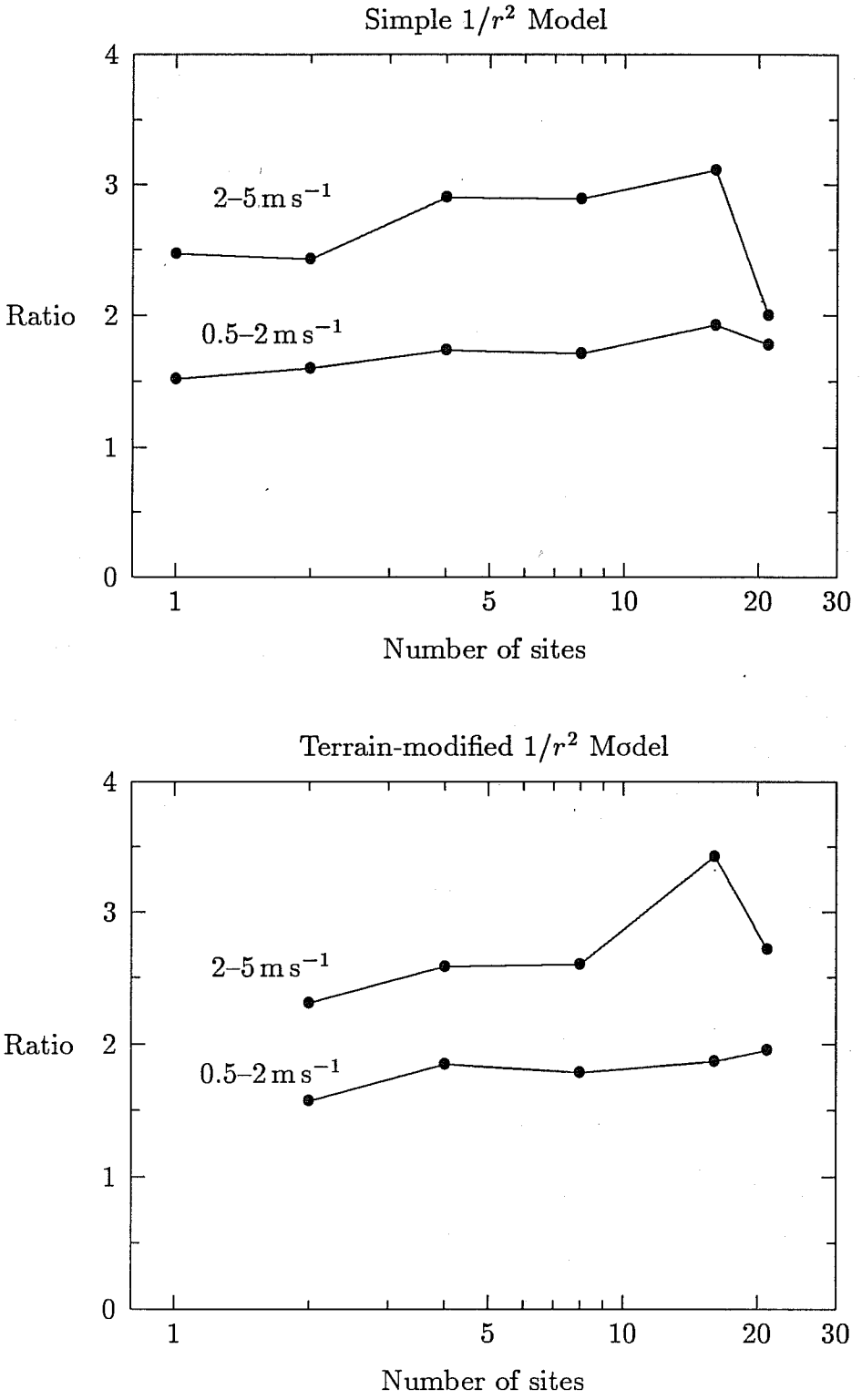

Fig. 18. The ratio of $\langle \gamma_r \rangle_N$ for the cross-valley component to $\langle \gamma_r \rangle_N$ for the along-valley component plotted as a function of the number of input sites. Separate curves are plotted for each wind-speed category.

The two interpolation models are compared in Fig. 19 by plotting the percentage difference between their values of $\langle \gamma_r \rangle_N$ at each N. Negative percentages indicate that the terrain-modified $1/r^2$ model has a smaller value of $\langle \gamma_r \rangle_N$ than the simpler model. A circle around a datum means that the 95% confidence interval for the datum does not overlap the 0% line. The figure indicates that adding more towers to the network improves the skill of the terrain-modified $1/r^2$ model more than that of the simpler model. At small values of N, the simple model actually seems to perform somewhat better for the highest speed category. But at $N = 16$, $\langle \gamma_r \rangle_N$ for the terrain-modified model is consistently lower.

7. CONCLUSIONS

The three Department of Energy plants on the Oak Ridge Reservation are in the process of upgrading and integrating their capability to respond to accidental releases of toxic materials. As part of this emergency-management project, the Atmospheric Turbulence and Diffusion Division has conducted a meteorological site survey of the Oak Ridge area. Twenty-eight meteorological towers were installed in the Oak Ridge area over a period from October 1989 to November 1990. Both one-minute and 15-minute averages of wind speed, wind direction, temperature, relative humidity, and rainfall were obtained from these towers.

This report presents a preliminary analysis of the site-survey wind data. A primary goal of this document is a recommendation to ORO on how many meteorological towers should permanently be installed in the Oak Ridge area. Because of time constraints, only a fraction of the available site-survey data was used in the analysis. A fuller analysis of the site-survey data could alter some of the conclusions and recommendations that are given in this report.

Eight-point wind roses were computed from a year of data at selected sites in the Oak Ridge tower network. These wind roses indicate that the terrain has a strong channeling effect on the winds in the Tennessee River Valley. The sites located on local ridge tops and in local valley bottoms have a high frequency of southwesterly and northeasterly winds, corresponding to the alignment of the Tennessee River Valley and the 100 m ridges that run along the bottom of the valley. In contrast, the wind roses at two Cumberland Mountain sites, which are not in the Tennessee River Valley, have frequent westerly winds but highly infrequent easterly winds. These stations more closely reflect the overall synoptic flow in Tennessee.

In addition to wind roses, cumulative frequency distributions of wind speed were computed for selected measurement towers. As expected, one of the Cumberland Mountain sites was the windiest, with wind speeds less than $5\,\mathrm{m\,s^{-1}}$ about 65% of the time. Within the Tennessee River Valley, speeds less than $5\,\mathrm{m\,s^{-1}}$ occurred more than

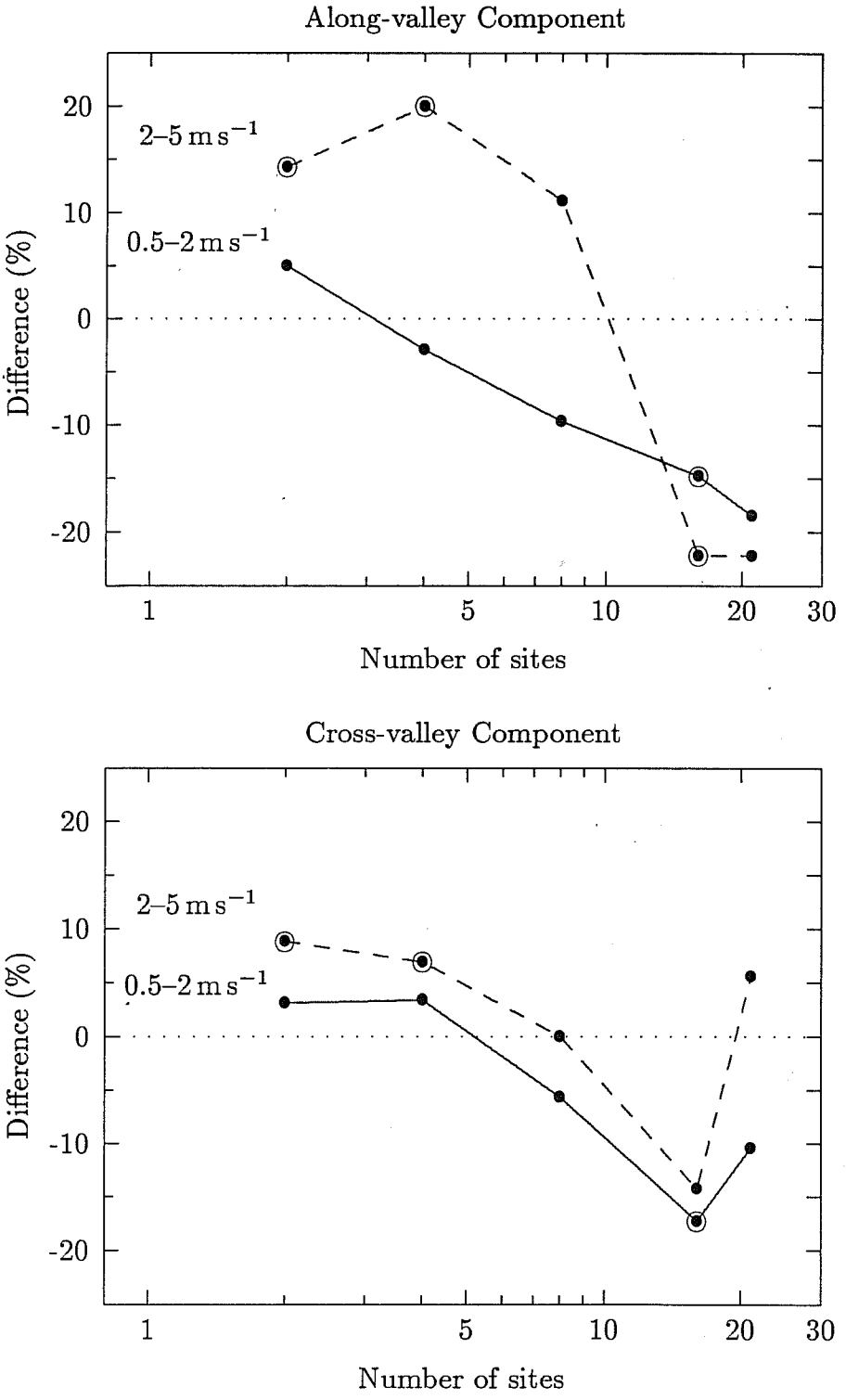

Fig. 19. Plots showing by what percentage the value of $\langle \gamma_r \rangle_N$ for the terrain-modified $1/r^2$ model differs from the corresponding value for the simple $1/r^2$ model. A circle around a data point indicates that the 95% confidence interval for the point does not overlap 0%.

90% of the time. At stations in the local valley bottoms, wind speeds less than $2\,m\,s^{-1}$ were present about 70% of the time.

To provide information on the degree of correlation among wind measurement sites, omnidirectional variograms were plotted for both the along-valley and cross-valley wind components. Many of the variograms have a large amount of scatter, so it is difficult to obtain solid conclusions. When wind speeds are greater than $2\,m\,s^{-1}$, the variograms suggest that site separations of about 10 km are sufficient to resolve the wind field in the valley bottoms. For wind speeds between 0.5 and $2\,m\,s^{-1}$, site separations of 6–8 km are adequate to resolve the along-valley wind component in the valley bottoms, but it may be impractical to resolve the cross-valley component in these light winds. The ridge-top variograms indicate that site separations of 16–18 km are sufficient in light winds (0.5–$2\,m\,s^{-1}$), but for winds greater than $5\,m\,s^{-1}$, separations of 40 km are adequate at ridge-top level.

The site-survey data were used to assess the performance of two wind-field interpolation models: a simple $1/r^2$ model and a terrain-modified $1/r^2$ model. Each model was evaluated using 2, 4, 8, 16, and 21 towers as input. Like the variogram analysis, the model evaluations suggest that an impractically large number of wind measurement sites would be required to adequately sample the cross-valley component in winds of less than $2\,m\,s^{-1}$. At higher wind speeds, around eight sites should be adequate for the cross-valley component. Approximately 16 sites are required to resolve the along-valley component in winds of 0.5–$2\,m\,s^{-1}$, but in stronger winds only a couple of sites should be adequate for this component.

Both interpolation models are better able to estimate the along-valley wind component than the cross-valley component. This is consistent with the results of the variogram analysis (*i.e.*, Table 4). For both interpolation models, increasing the number of wind input sites improved the estimates of the along-valley component more than those of the cross-valley component. This is another indication that even in strong winds the cross-valley component is significantly influenced by local wind-flow features.

The conclusions resulting from the variogram analysis and the model evaluations should be taken as general guidelines and not as rigid dogma. Atmospheric researchers have only recently started to investigate the spatial variability of wind fields in complex terrain, so a considerable amount of work remains. Future research will likely provide more precise guidelines for the measurement and modeling of wind fields in complex terrain.

8. RECOMMENDATIONS

We recommend that ten meteorological towers be installed in the Oak Ridge area to provide adequate coverage of the regional-scale wind field. These towers are intended

to supplement the measurements that are already being taken at the three ORO plants. Table 7 specifies the recommended locations for the supplemental towers. Only locations where ATDD had an operating tower during the site survey are included in Table 7, because we have some knowledge of the wind flow at these sites.

Five of the recommended towers are on ridge tops, and four are in valley bottoms. The ridge-top sites have an average separation of about 20 km, which is close to the 16–18 km limit indicated for light-winds in Table 4. The average separation of the valley-bottom sites—including the measurements taken at the ORO plants—is about 8 km; this is within the 6–8 km light-wind limit for the along-valley component and the 10 km moderate-wind limit for the cross-valley component that are indicated in Table 4. A total of 12 measurement sites (excluding site BU) in the Oak Ridge area is also a reasonable compromise of the numbers in Table 6.

Table 7. Recommended locations for supplemental meteorological towers in the Oak Ridge area

		UTM (km)	
Abbreviation	Name	Easting	Northing
	Valley-bottom sites		
EF	East Fork	739.70	3983.80
LV	Lawnville valley	730.80	3975.20
OR	ORAU	746.69	3988.31
PS	Pellissippi State	755.92	3981.62
	Ridge-top sites		
BR	Bluebird Ridge	764.15	4003.23
K25	K-25 ridge top	732.00	3979.80
LC	Lenoir City	741.00	3969.31
SR	Sharp's Ridge	775.40†	3988.23†
WB	Walker Branch	744.62	3982.62
	Cumberland Mountain site		
BU	Buffalo Mountain	739.77	3999.23

† SR is actually in UTM zone 17 at 234.55 km easting and 3987.54 km northing.

Site BU is included in the supplemental-tower list to provide information about the wind flow above the Tennessee River Valley. These upper-level data may be useful for elevated contaminant releases and for estimating contaminant transport out of the Tennessee River Valley. Such data may also aid more sophisticated numerical models in creating a three-dimensional wind field for the Oak Ridge area.

Table 7 is intended to indicate the general locations for the supplemental measurements, not precise coordinates that must be rigidly followed. The final locations for the supplemental towers may be adjusted somewhat because of practical or logistical constraints. We recommend, however, that ATDD be consulted before final locations are approved.

ACKNOWLEDGMENTS

This report was prepared as part of the Emergency Management Program at the Atmospheric Turbulence and Diffusion Division. The program is funded by and provides guidance to the Department of Energy's Oak Ridge Operations. The authors would like to acknowledge the contribution of J. R. White, who supervised and maintained the tower network around Oak Ridge. We are also grateful to J. Gholston, M. E. Hall, J. D. Womack, and J. Wynn for providing assistance during the site survey.

REFERENCES

ATDD (Atmospheric Turbulence and Diffusion Division), 1991. HARM-II User's Guide. M. S. Waugh (Ed.), NOAA/ATDD, Oak Ridge, Tenn., 132 pp.

Cressman, G. P., 1959. An operational objective analysis system. *Mon. Weather Rev.*, **87**:367–374.

Eckman, R. M., 1990. The suitability of dense-contaminant models for emergency preparedness systems. NOAA Tech. Memo. ERL ARL-182, NOAA Air Resources Laboratory, Silver Spring, Md., 19 pp.

Eckman, R. M. and R. J. Dobosy, 1989. The suitability of diffusion and wind-field techniques for an emergency-response dispersion model. NOAA Tech. Memo. ERL ARL-171, NOAA Air Resources Laboratory, Silver Spring, Md., 28 pp.

Goodin, W. R., G. J. McRae, and J. H. Seinfeld, 1979. A comparison of interpolation methods for sparse data: application to wind and concentration fields. *J. Appl. Meteorol.*, **18**:761–771.

Guo, X. and J. P. Palutikof, 1990. A study of two mass-consistent models: problems and possible solutions. *Boundary-Layer Meteorol.*, **53**:303–332.

Hanna, S. R., G. A. Briggs, and R. P. Hosker, Jr., 1982. Handbook on Atmospheric Diffusion. DOE/TIC-11223, Technical Information Center, U. S. Dept. of Energy, 102 pp.

Isaaks, E. H. and R. M. Srivastava, 1989. *Applied Geostatistics.* Oxford University Press, New York, 561 pp.

Journel, A. G. and C. J. Huijbregts, 1978. *Mining Geostatistics.* Academic Press, London, 600 pp.

Lange, R., 1989. Transferability of a three-dimensional air quality model between two different sites in complex terrain. *J. Appl. Meteorol.*, **28**:665–679.

Lanicci, J. M. and H. Weber, 1986. Validation of a surface-layer windflow model using climatology and meteorological tower data from Vandenberg AFB, California. AFGL-TR-86-0210, Air Force Geophysics Laboratory, Hanscom AFB, Mass., 88 pp.

Nappo, C. J., 1977. Mesoscale flow over complex terrain during the Eastern Tennessee Trajectory Experiment (ETTEX). *J. Appl. Meteorol.*, **16**:1186–1196.

Pendergrass, W. R., 1989. Meteorological site survey of the Feed Materials Production Center, Fernald, Ohio. ATDD Contribution no. 89/2, NOAA Atmospheric Turbulence and Diffusion Division, Oak Ridge, Tenn., 41 pp.

Pendergrass, W. R., 1990a. Meteorological site survey of the Paducah Gaseous Diffusion Plant, Paducah, Kentucky. ATDD Contribution no. 91/22, NOAA Atmospheric Turbulence and Diffusion Division, Oak Ridge, Tenn., 46 pp.

Pendergrass, W. R., 1990b. Meteorological site survey of the Portsmouth Gaseous Diffusion Plant, Portsmouth, Ohio. ATDD Contribution no. 91/23, NOAA Atmospheric Turbulence and Diffusion Division, Oak Ridge, Tenn., 50 pp.

Ross, D. G. and I. N. Smith, 1986. Diagnostic wind field modelling for complex terrain: testing and evaluation. CAMM report no. 5/86, Chisholm Institute of Technology, Caulfield East, Australia, 93 pp.

U. S. Weather Bureau, 1953. A meteorological survey of the Oak Ridge area. ORO-99, Office of Technical Services, U. S. Dept. of Commerce, Washington, D. C., 584 pp.

Wendell, L. L., 1972. Mesoscale wind fields and transport estimates determined from a network of wind towers. *Mon. Weather Rev.*, **100**:565–578.

APPENDIX: SITE-SURVEY CHANNEL NUMBERS

Table 8. List of radio-frequency channel numbers used during the Oak Ridge site survey

Channel number	Description
1	Data from site AT1
2	Data from site CF
3	Data from site LA
4	Data from site FB
5	Data from site BU
6	Data from site SA
7	Data from site AT2
8	Data from site K25
9	Data from site SR
11	Data from site WP
12	Data from site LC
13	Data from site BR
14	Data from 15 m level at site FH
15	Data from site SC
16	Data from 21 m level at site FH
18	Combined data from 11, 30, and 46 m levels at site BT
19	Data from site WB
20	Data from site 8A
21	Combined data from 53, 76, and 95 m levels at site BT
22	Data from site OR
23	Data from site PS
24	Data from site KR
25	Data from site LV
26	Data from site 25R
27	Data from site MH
28	Data from site PV
29	Data from site PC
30	Data from site KI
31	Data from site EF
47	Data from site X10
71	Data from 53 m level at site BT
78	Data from 11 m level at site BT
81	Data from 76 m level at site BT
88	Data from 30 m level at site BT
91	Data from 95 m level at site BT
98	Data from 46 m level at site BT

☆ U.S. GOVERNMENT PRINTING OFFICE 1992–628-432/40074